OUKA
Osaka University Knowledge Archive

Title	Retinal metabolism in rod and cone photoreceptors
Author(s)	宮園, 貞治
Citation	大阪大学, 2008, 博士論文
Version Type	VoR
URL	https://doi.org/10.18910/49333
rights	
Note	

Osaka University Knowledge Archive : OUKA

https://ir.library.osaka-u.ac.jp/

Osaka University

Doctor Thesis

Retinal metabolism in rod and cone photoreceptors

(桿体と錐体におけるレチナール代謝)

Sensory Transduction Group (Prof. Kawamura)
Nanobiology Laboratories
Graduate School of Frontier Biosciences
Osaka University

Sadaharu Miyazono

September 2008

論　文　内　容　の　要　旨

Retinal metabolism in rod and cone photoreceptors.
（桿体と錐体におけるレチナール代謝）

脊椎動物の網膜には、桿体、錐体の２種類の視細胞が存在する。桿体は光に対する感度が高いため暗所で働き、錐体は光に対する感度が低いため明所で働く。どちらの視細胞も、視物質によって光を受容し、それを細胞の電気応答に変換する。視物質は、発色団である11-*cis* retinalと蛋白質オプシンから構成される。11-*cis* retinalが光を受容するとall-*trans* retinalに異性化し、オプシンに構造変化をもたらして視物質は活性型になる。その結果、光情報伝達機構が活性化されて、視細胞が電気応答を発生する。異性化したall-*trans* retinalはしばらくするとオプシンから外れる。オプシンは11-*cis* retinalと結合することによって初めて光を受容することができる。そのため、all-*trans* retinalは、網膜内のretinal代謝経路により11-*cis* retinalに戻され、オプシンと再び結合し、視物質が再生する。錐体は明所で働くため、暗所で働く桿体より視物質消費量が多い。そのため、視物質代謝、すなわちretinal代謝は桿体に比べ、錐体でより高効率であると予想される。これまでretinal代謝については、桿体での研究が先行しており、錐体での研究はほとんど行われてこなかった。なぜなら、桿体は大量に精製できるので生化学的な研究が可能であったが、錐体の精製は難しいため研究が進展しなかったからである。当研究室には、世界で唯一錐体視細胞を大量に精製する技術があるので、錐体の生化学的な研究が可能である。そこで、両者のretinal代謝を生化学的に比較することにした。

光により生じたall-*trans* retinalは視細胞内でall-*trans* retinolに還元される。まず、精製した桿体、錐体細胞全体を用いた実験から、この還元活性は錐体では桿体に比べて８倍程度高いことが分かった。ところで、桿体、錐体ともに、外節と内節と呼ばれる部分からなる。視物質は外節に含まれるので、all-*trans* retinalの還元活性は外節に局在すると予想される。そこで、外節に局在する活性を求めるために、桿体、錐体の両方について外節もしくは内節を多く含む試料を調製した。これを用いた実験により、桿体には内節にも高い活性があること、一方錐体には外節に高い活性があることが分かり、外節だけで比較すると、錐体では桿体に比べて活性が約３３倍高いことが分かった。さらに、この活性は桿体、錐体ともにretinol dehydrogenase ８（RDH８）によるものであり、錐体で高い活性を示すのはRDH８が錐体外節に大量に発現しているからであった。以上のことから、錐体では光受容により生じたall-*trans* retinalを素早く除去できることが示唆された。

一方、視物質が再生されるためには、11-*cis* retinalが供給されなければならない。retinal代謝経路において、錐体には11-*cis* retinolが供給されると考えられており、錐体内で11-*cis* retinolが11-*cis* retinalに変換されると考えられている。この反応は補酵素$NADP^+$の還元と共役したRDHの反応であると考えられていた。しかし、精製した錐体にはそのような活性はほとんど認められなかった。retinolをretinalに変換する反応は酸化反応であり、この反応には$NADP^+$のような酸化剤の還元が必ず共役する。そこで、酸化剤の候補としてall-*trans* retinalを考えた。all-*trans* retinalは光受容により視物質から放出される。11-*cis* retinolとall-*trans* retinalを加えた錐体試料では予想通り11-*cis* retinalとall-*trans* retinolが生じた。そして、この反応は、RDHの反応に比べて約５０倍高い活性を示した。以上のことから、この反応を触媒する分子（または分子群）は未同定ではあるものの、この反応は錐体での視物質再生に非常に重要な役割を果たすことが示唆された。

Contents

Summary

In the vertebrate retina, there are two types of photoreceptors, rods and cones. Rods mediate twilight vision and cones mediate daylight vision. In both cells, photons are absorbed by visual pigment, which is composed of a chromophore, 11-*cis* retinal and a protein moiety, opsin. Light isomerizes 11-*cis* retinal to all-*trans* retinal, which induces a conformational change in opsin to lead to activation of an enzymatic cascade to evoke a light response. All-*trans* retinal, the product formed after light-absorption, then dissociates from opsin, and is reduced to all-*trans* retinol in the photoreceptor outer segment. Opsin molecules without chromophore are no longer able to absorb photons in the visible region. To form functional pigment again, opsin must newly bind 11-*cis* retinal. It is known that all-*trans* retinol is converted back to 11-*cis* retinal through a multistep pathway, and is supplied to opsin to regenerate visual pigment. Because cones function under much brighter light conditions, retinal metabolism, i.e., reduction of all-*trans* retinal and production of 11-*cis* retinal, could be more efficient in cones than in rods to regenerate pigment effectively.

In the present study, by using carp purified rods and cones, first I compared the reduction of all-*trans* retinal to all-*trans* retinol by retinol dehydrogenases (RDHs) between rods and cones. The activity in the outer segment of cones was >30 times higher than that of rods. The high activity of RDHs was attributed to a higher content of RDH8 in cones. I further found a novel and effective pathway to convert 11-*cis* retinol to 11-*cis* retinal in cones: this oxidative conversion did not require $NADP^+$, and instead, was coupled with reduction of all-*trans* retinal to all-*trans* retinol. The activity was >50 times more effective than the reaction that requires $NADP^+$. These highly effective reactions of removal of all-*trans* retinal and production of 11-*cis* retinal are probably the underlying mechanisms that ensure effective pigment regeneration in cones that function under much brighter light conditions than rods.

Introduction

We can see the external world under light conditions that range from dim starlight to bright sunlight, where the difference of light intensity is almost a thousand-million-fold. Our eyes have an ability to detect light signals of various intensities. For this ability, in the vertebrate retina, there are two types of photoreceptor cells, rods and cones (Figure 1). Rods are very light-sensitive so that they function under dim light. Cones are less light-sensitive so that they function under bright light. Thanks to these two types of photoreceptors, the dynamic range of our visual system is very wide.

Both rods and cones consist of the outer segment (OS) and the inner segment (IS) that includes the nucleus region and synaptic region (Figure 2A). The OS contains the components necessary for conversion of a light signal to an electrical signal, and the IS contains organelles necessary for general cell metabolism, such as nucleus and mitochondria. Rods and cones are distinguishable by their shapes of the OS. In rods, about

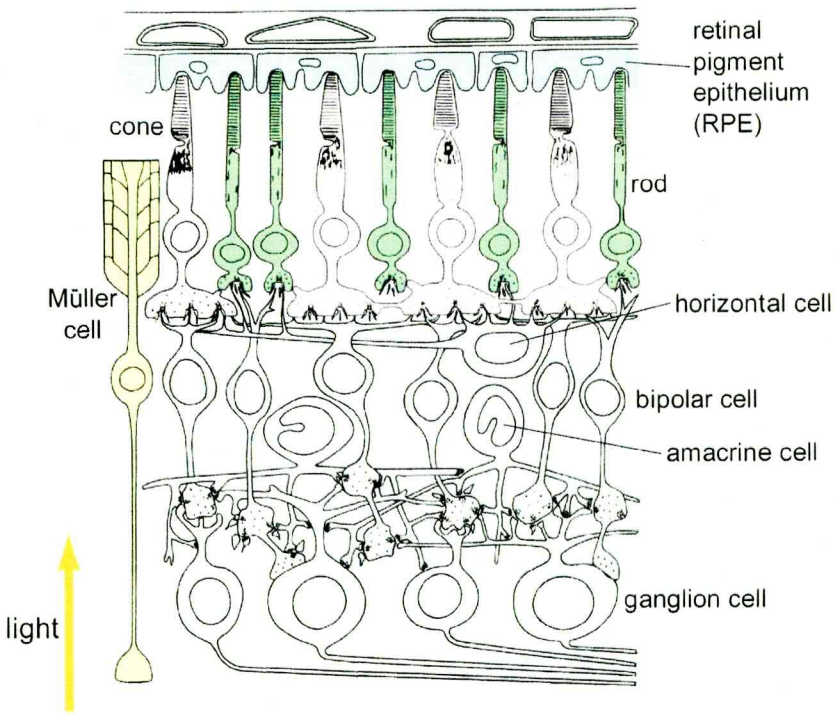

Figure 1. Vertebrate retina. Vertebrate retina contains several species of cells. Among them, there are two types of photoreceptors, rods (green) and cones (pink). Modified from Dowling and Boycott (1966).

1000 disk membranes are stacked inside of the OS, and in cones, the plasma membranes are invaginated repeatedly to form a stack of lamellar structure. Visual pigment is present in the stacked membranes of the OS, and the molecule is packed at a very high density (~3mM) (Harosi, 1975). This dense packing serves to increase the probability of absorption of photons that are transmitted through the OS in parallel with its long axis.

Visual pigment is one of the G protein-coupled receptor proteins and composed of a chromophore and a protein moiety, called opsin (Gether, 2000; Stenkamp et al., 2005) (Figure 2B). The light-absorbing chromophore is 11-*cis* retinal, a derivative of vitamin A. Light isomerizes 11-*cis* retinal to all-*trans* retinal. This isomerization of the chromophore induces a conformational change in opsin to lead to activation of an enzyme cascade to evoke an electrical response of a photoreceptor. This enzyme cascade is called phototransduction cascade (outlined by a red dotted line in Figure 2B). All-*trans* retinal, the product formed after light-absorption, then dissociates from opsin, and is converted back to 11-*cis* retinal through a multistep pathway, and is supplied to opsin to regenerate visual pigment. This process is called visual cycle (outlined by a blue dotted line in Figure 2B).

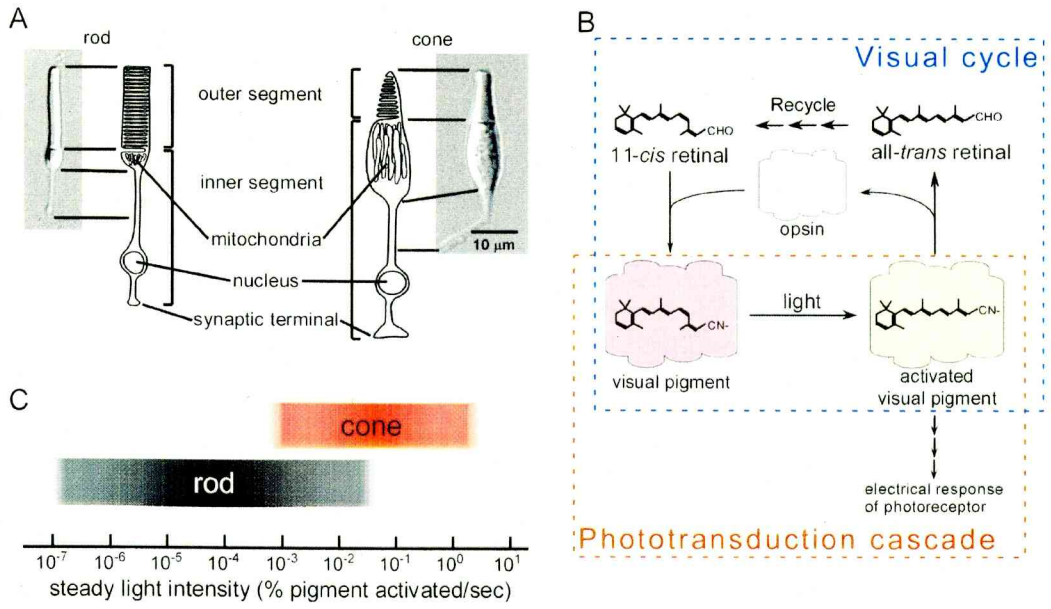

Figure 2. Rods and cones. (A) A rod and a cone brushed off the carp retina. Both cells consist of two parts, the outer segment and the inner segment. (B) Phototransduction cascade and visual cycle. Visual pigment consisting a part of the phototransduction cascade is recycled in the visual cycle. (C) Intensity of steady light under which rods and cones can function. Estimated from Baylor et al. (1984), Schnapf et al. (1990), Mendez et al. (2001) and Calvert et al. (2002).

Rods and cones are different in their characteristics of photoresponse. Cones can function under brighter light condition than rods (Figure 2C). The light sensitivity of rods is 10^2-10^3 times higher than that of cones, and further, each rod or cone covers about a 10^3-fold range of the light-intensity. The presence of both rods and cones ensure the coverage of the wide range of light-intensities in our vision. Rods mediate twilight vision because of their high light-sensitivity. Cones mediate daylight vision, because they are less sensitive to light.

The phototransduction cascade to generate a photoresponse in rods is well understood (Figure 3) (Burns and Arshavsky, 2005; Lamb and Pugh, 2006; Fu and Yau, 2007). In rods, a photon activates a visual pigment molecule. The activated visual pigment activates a GTP-binding protein, transducin, by substitution of GTP for GDP. Activated transducin activates cGMP phosphodiesterase (PDE) that hydrolyzes cGMP. As a result, the cGMP concentration is decreased in the light. Finally, the decrease of the cGMP concentration induces the closure of cGMP-gated cation channels present in the plasma membrane of the OS. The phototransduction mechanisms have been known to be similar

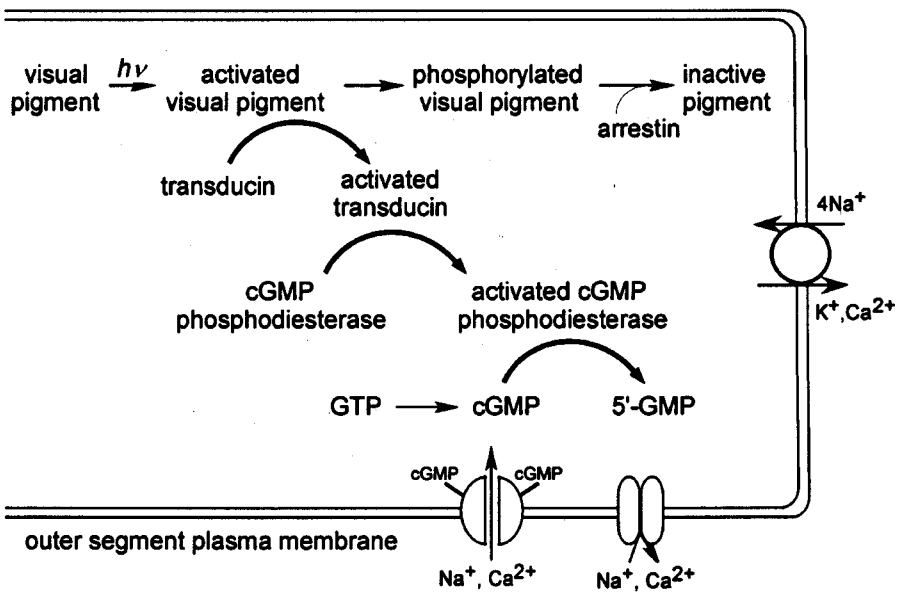

Figure 3. Phototransduction cascade in the vertebrate rods and cones. In the outer segment of rods and cones, cGMP is hydrolyzed light-dependently through this cascade (see details in text). Modified from Figure 2 in Kawamura and Tachibanaki (2008).

in rods and cones. The detailed mechanisms responsible for the difference in light-sensitivity in rods and cones are now understood well at the molecular level (Tachibanaki et al., 2007; Kawamura and Tachibanaki, 2008).

When visual pigment absorbs light, the chromophore is isomerized to all-*trans* form and sequentially becomes apart from opsin. Because retinal is a toxic form of retinoids (Weng et al., 1999), all-*trans* retinal has to be rapidly removed. It is known that all-*trans* retinal is reduced to all-*trans* retinol by retinol dehydrogenases (RDHs) within the OS of a photoreceptor. Because cones function under much brighter light conditions, the reduction of all-*trans* retinal would be more efficient in cones than in rods. Recently, the rate of the reduction has been reported to be 10-40 times higher in cones than in rods under *in vivo* conditions (Ala-Laurila et al., 2006). Yet, the molecular basis is not known.

Visual pigment without chromophore is no longer able to absorb light. To form functional visual pigment again, opsin needs to bind 11-*cis* retinal. To supply 11-*cis* retinal, it is known that all-*trans* retinal released from opsin is converted back to 11-*cis* retinal through a multistep pathway. This process is called visual cycle that requires participation of the retinal pigment epithelium (RPE) (Figure 4, upper left) (McBee et al., 2001; Lamb and Pugh, 2004). In the visual cycle, as described above, all-*trans* retinal released from visual pigment is reduced to all-*trans* retinol within a photoreceptor. All-*trans* retinol is then transported to the RPE. In the RPE, there are three steps of reactions of the visual cycle. First, all-*trans* retinol is esterified to form an all-*trans* retinyl ester by lecithin retinol acyl transferase (LRAT). The second reaction couples hydrolysis of the retinyl ester with the isomerization of all-*trans* retinol to 11-*cis* retinol catalyzed by retinyl ester isomerohydrolase, RPE65. Finally, 11-*cis* retinol is oxidized to 11-*cis* retinal by 11-*cis* retinol dehydrogenase (RDH5). The newly synthesized 11-*cis* retinal is sent back to photoreceptors to regenerate visual pigment.

All the above studies were performed in the rod-dominant retina. Because cones function under much brighter light conditions, the supply of 11-*cis* retinal to regenerate visual pigment could be faster in cones. Several lines of evidence suggested that cone pigment is regenerated in an RPE-independent manner. For example, cone pigment, but not rod pigment, can be regenerated in isolated frog retinas separated from the RPE (Goldstein and Wolf, 1973). Interestingly, after bleaching, photosensitivity recovers with

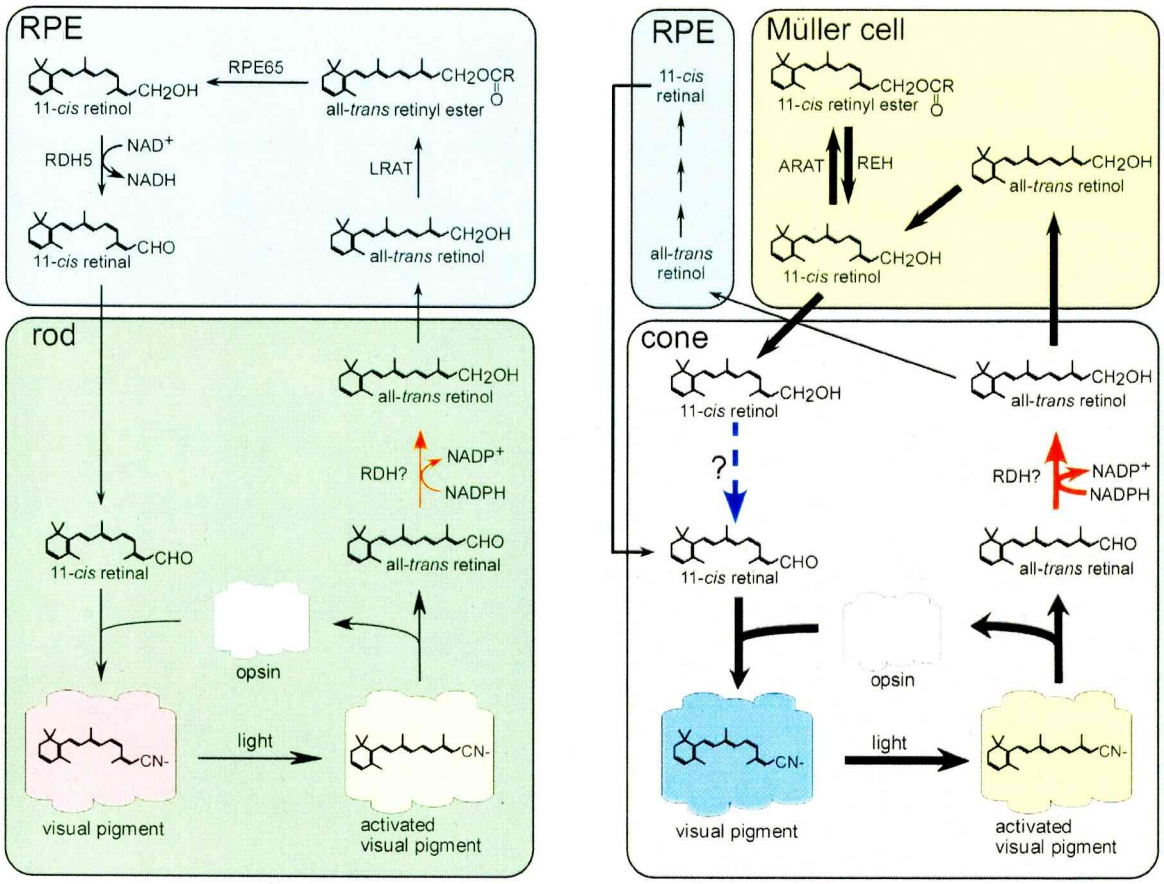

Figure 4. Scheme of rod and cone visual cycle. (Left) Currently supported visual cycle for rods. After absorption of light, the visual pigment chromophore, 11-*cis* retinal is isomerized to all-*trans* reteinal. All-*trans* retinal is detached from opsin and reduced by RDHs to all-*trans* retinol in the presence of a cofactor, NADPH. This retinol is transferred to the RPE where the all-*trans* form is isomerized to the 11-*cis* form and is oxidized to 11-*cis* retinal. 11-*cis* retinal is transferred back to the OS of a rod to regenerate visual pigment. (Right) Hypothetical visual cycle for cones. A similar pathway of visual cycle is present in cones. In cones, additional pathway for its supply is assumed to be present and much effective: 11-*cis* retinol supplied from Müller cells is converted to 11-*cis* retinal by hypothesized enzyme, 11-*cis* retinol dehydrogenase with a cofactor, $NADP^+$. See text for details.

addition of 11-*cis* retinol in isolated cones, but not in rods (Jones et al., 1989). In addition, cultured Müller cells, the major glial cells, can isomerize all-*trans* retinol to 11-*cis* retinol (Das et al., 1992). Recently, it has been hypothesized that an effective pathway for supply of 11-*cis* retinol to cones is present in isolated cone-dominant, chicken and ground squirrel retinas (Figure 4, upper right, Mata et al., 2002). However, it is not known whether the Müller cells have this effective pathway because Mata et al. used cone-dominant retina, but not purified Müller cells. Similar to the rod visual cycle in cones, 11-*cis* retinal in the cone visual pigment is isomerized to all-*trans* retinal by light, and then all-*trans* retinal is assumed

to be reduced to all-*trans* retinol by unidentified RDHs (Muniz et al., 2007). In the hypothesis proposed by Mata et al. (2002), all-*trans* retinol is transported to Müller cells, can be isomerized to its 11-*cis* form as a result of the synthesis of 11-*cis* retinyl ester by 11-*cis* acyl CoA retinol acyl transferase (ARAT), and then 11-*cis* retinyl ester is hydrolyzed to 11-*cis* retinol by retinyl ester hydrolase (REH). This isomerization of all-*trans* form to 11-*cis* form in the Müller cells has been reported to be 20 times more effective than in the RPE (Mata et al., 2002). It is further assumed that this 11-*cis* retinol is transported to cones, and is oxidized to 11-*cis* retinal by a hypothesized enzyme, 11-*cis* retinol dehydrogenase that is present in cones and requires $NADP^+$ as a cofactor. This oxidation pathway must be also effective for regeneration of cone pigment, if it is present.

In the present study, I investigated the metabolism of all-*trans* rertinal and 11-*cis* retinal within the photoreceptor cells (Figure 3, red and blue arrows). By using purified carp (*Cyprinus carpio*) rods and cones together with the outer segment (OS)- and the inner segment (IS)-rich rod and cone preparations, I first measured the activity of the reduction of all-*trans* retinal (RDH activity) in the OS and the IS of both rods and cones. The result showed that the activity is ~30 times higher in the OS in cones than in rods. I then quantified the specific activities and the amount of the major RDHs (RDH8, RDH8L2 and RDH13) expressed in the photoreceptors. From these studies, I concluded that the high activity of RDHs in the cone OS is attributed to high content of RDH8 in the OS of cones. Furthermore, I found a novel reaction for the effective conversion of 11-*cis* retinol to 11-*cis* retinal in cones. This reaction does not require $NADP^+$, a cofactor that has been thought to be essential for retinol oxidation. Instead, 11-*cis* retinal was produced by a novel enzymatic reaction in which the reduction of all-*trans* retinal and the oxidation of 11-*cis* retinol are couplied (retinal-retinol redox coupling reaction; ALOL-coupling). I propose that this oxidation pathway becomes effective when the light intensity increases to accumulate a large amount of all-*trans* retinal in the cone OS.

Results

All-*trans* Retinal Reduction is More Efficient in Cones

All-*trans* retinal formed by absorption of light in visual pigment is reduced to all-*trans* retinol in the photoreceptor cells. To compare the reducing activities between rods and cones, I first purified rods and cones from the carp retina (see Experimental Procedures). Briefly, rods and cones were brushed off the retina (Figure 5A). The cells were purified by using a stepwise Percoll density gradient. Rods were collected at the 45/60% (w/v) interface (Figure 5B), and cones were collected at the 75/90% (w/v) interface (Figure 5C). Our rod preparation contained small amounts of cones (Tachibanaki et al., 2001).

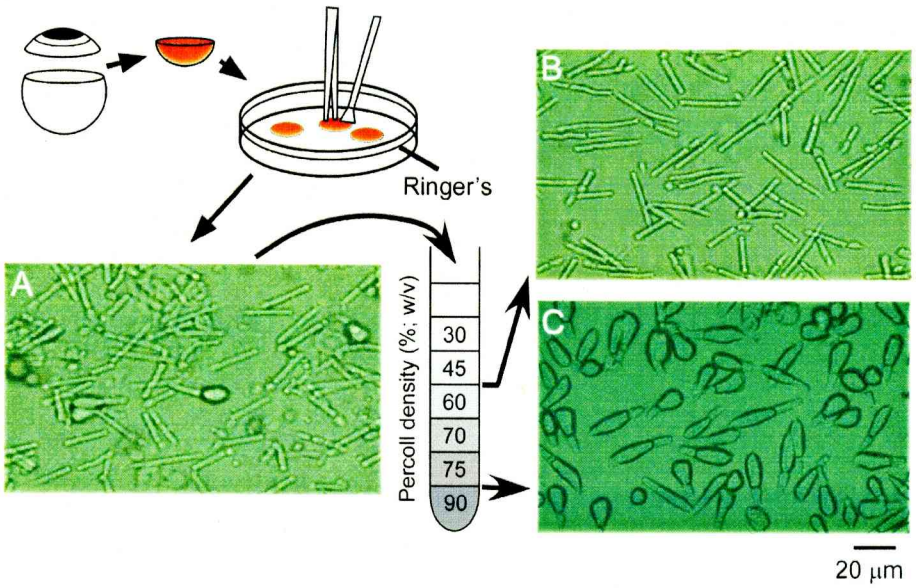

Figure 5. Purification of rods and cones from the carp retina. (A-C) Rods and cones were brushed off the retina (A). The mixture of rods and cones was layered on the top of a stepwise Percoll density gradient. After centrifugation, rods were obtained at the 45/60% interface (B), and cones were obtained at the 75/90% interface (C). Modified from Figure 1 in Tachibanaki et al. (2001).

In Figure 6A, the reaction products were analyzed by HPLC. Figure 6B shows the time courses of the reduction of the exogenously applied all-*trans* retinal to all-*trans* retinol measured in the lysate of purified carp rods and cones. I routinely quantified the amount of rods and cones by measuring the amount of visual pigment in a sample. Therefore, the activity of the reduction of all-*trans* retinal, defined as the RDH activity in this study, was

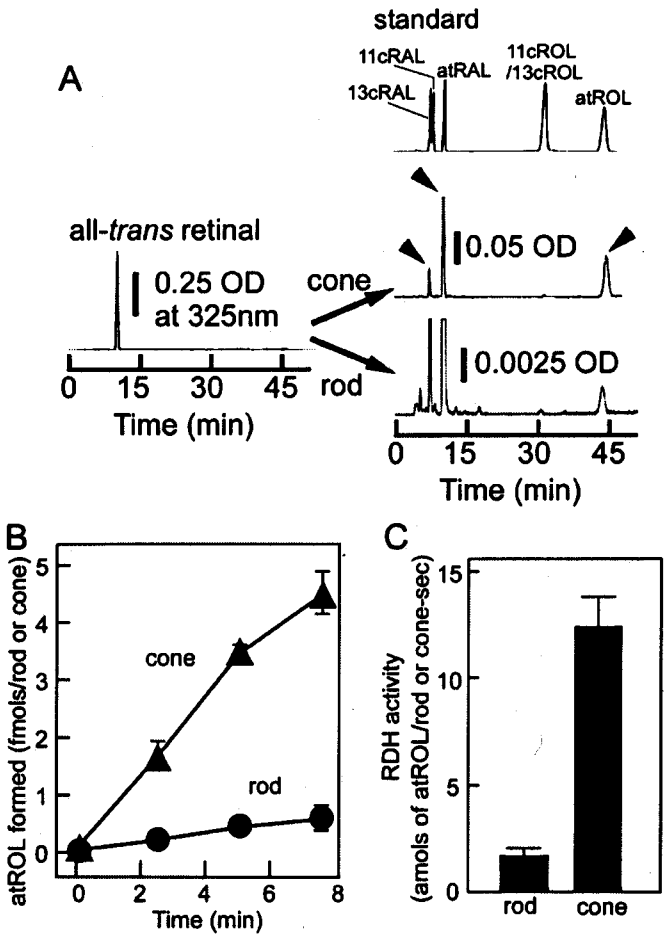

Figure 6. RDH activities in purified rods and cones. (A) HPLC elution patterns of retinoids after incubation of all-*trans* retinal (left) with cone (middle right) and rod (lower right) lysate. (upper right) A representative HPLC chromatogram of retinal and retinol standards: 13-*cis* retinal (13cRAL), 11-*cis* retinal (11cRAL), all-*trans* retinal (atRAL), 11-*cis* retinol (11cROL), 13-*cis* retinol (13cROL) and all-*trans* retinol (atROL).Arrowheads in the middle right panel indicate (from left to right) 13-*cis* retinal, all-*trans* retinal and all-*trans* retinol. Formation of 13-*cis* retinal is due to thermal isomerization from all-*trans* retinal (see Figure 18B). (B) Time course of reduction of all-*trans* retinal (RDH activity) in the rod and the cone lysate. The activity is expressed as fmols of all-*trans* retinol formed per cell. The abscissa indicates the time after addition of all-*trans* retinal. Error bars show standard deviations (n=4). (C) RDH activities in the rod and the cone lysate. The activity was calculated from the results at 5 min in (B) (n=4).

measured in units of per visual pigment present. This expression is useful in the comparison of the RDH activities per unit volume of the OS between rods and cones, because the density of the visual pigment in the OS is similar between rods and cones (Harosi, 1975). However, most of our purified rods and cones retained both the OS and the IS (see Experimental Procedures), and in addition, both the OS and the IS showed the RDH activity (see below). For this reason, I show the activity in units per cell (rod or cone)

by assuming that, on an average, a rod contains 1.6×10^8 and a cone contains 7.8×10^7 visual pigment molecules (Tachibanaki et al., 2001) until it becomes clear how much percent of the activity is present in the OS (after Figure 11).

As shown in Figure 6B, the rate of formation of retinol was higher in cones than that in rods. The RDH activity in rods was 1.6 ± 0.2 amols of all-*trans* retinol formed per cell per second (amols atROL/cell-sec) (Figure 6C). A similar value of the RDH activity has been reported in bovine rod outer segment (Palczewski et al., 1994). The activity in cones was 12.4 ± 1.4 amols atROL/cell-sec (Figure 6C). It was evident that the reducing activity per cell was ~8 times higher in cones.

The reduction of all-*trans* retinal is catalyzed by retinol dehydrogenases (RDHs) (Futterman, 1963; Palczewski et al., 1994; Rattner et al., 2000). To characterize the RDH reactions in rods and cones, I examined the substrate specificity of the oxidation and the reduction of retinoids (Figure 7A and 7B). For the measurement of the RDH activity (reduction of retinal to retinol), purified all-*trans* or 11-*cis* form of retinal was used as the substrate in the presence of NADPH, the essential cofactor of this reaction (Futterman, 1963; Nicotra and Livrea, 1982; Palczewski et al., 1994). For the measurement of the back reaction (oxidation of retinol to retinal), purified all-*trans* or 11-*cis* form of retinol was used as the substrate, and $NADP^+$ was used as the cofactor (Nicotra and Livrea, 1982; Palczewski et al., 1994). This was the first biochemical measurement of the RDH activities in purified cone preparations, although some attempts were made previously using the cone-dominant retina (Mata et al., 2002). All-*trans* retinal was the best substrate among the substrates examined for RDHs in both rods and cones, because the rate of the reduction of all-*trans* retinal was the highest. The activity of each reaction in cones was 3-8 times higher than that of the corresponding reaction in rods (compare Figure 7A and 7B). However, the dissociation constant (Kd) of each retinoid was similar between rods and cones. This result suggested that same RDH proteins are expressed in rods and cones. It should be mentioned here that in both rods and cones, the catalytic activity of the formation of 11-*cis* retinal from 11-*cis* retinol is remarkably lower than the activities of other reactions even in the presence of cofactors.

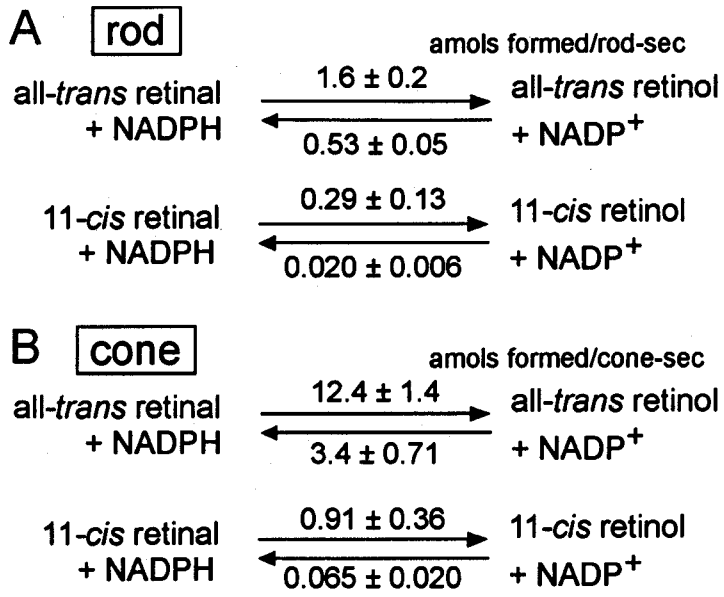

Figure 7. Activities of reduction and oxidation of all-*trans* and 11-*cis* retinoids in rods (A) and cones (B) lysate. The activity was measured in the presence of 100 μM retinal or retinol and 200 μM NADPH or $NADP^+$. The values are shown as a mean ± SD determined in four independent experiments for the all-*trans* retinoids and three independent experiments for the 11-*cis* retinoids.

RDH activities are present in Both Photoreceptor Outer Segments and Inner Segments

All-*trans* retinal is released after light-absorption from visual pigment that locates in the OS almost exclusively. Thus, all-*trans* retinal mainly accumulates within the OS, and its reduction to all-*trans* retinol is thought to predominantly take place within the OS. Actually, it has been reported that RDH proteins were expressed in both the OS and the IS in rods and cones, but that, in isolated rods and cones, the reduction of all-*trans* retinal to all-*trans* retinol was observed in the OS (Haeseleer et al., 1998; Rattner et al., 2000; Haeseleer et al., 2002; Ala-Laurila et al., 2006).

To investigate whether my measured RDH activity localizes only in the OS of rods and cones, I obtained outer segment (OS)-rich and inner segment (IS)-rich preparations of rods and cones (see Experimental Procedures). Briefly, purified rods (Figure 8A) were passed through a needle several times to mechanically detach the OS from the IS (Figure 8B) and fractionated with the use of a stepwise Percoll density gradient. A ROS-rich sample was obtained at the 30/45% (w/v) interface (Figure 8C), and a RIS-rich sample was

obtained at the 45/60% (w/v) interface (Figure 8D). Similarly, purified cones (Figure 8E) were passed through a needle to mechanically detach the OS from the IS (Figure 8F). After centrifugation, a COS-rich sample was obtained as the supernatant (Figure 8G), and a CIS-rich sample was obtained as the precipitate (Figure 8H).

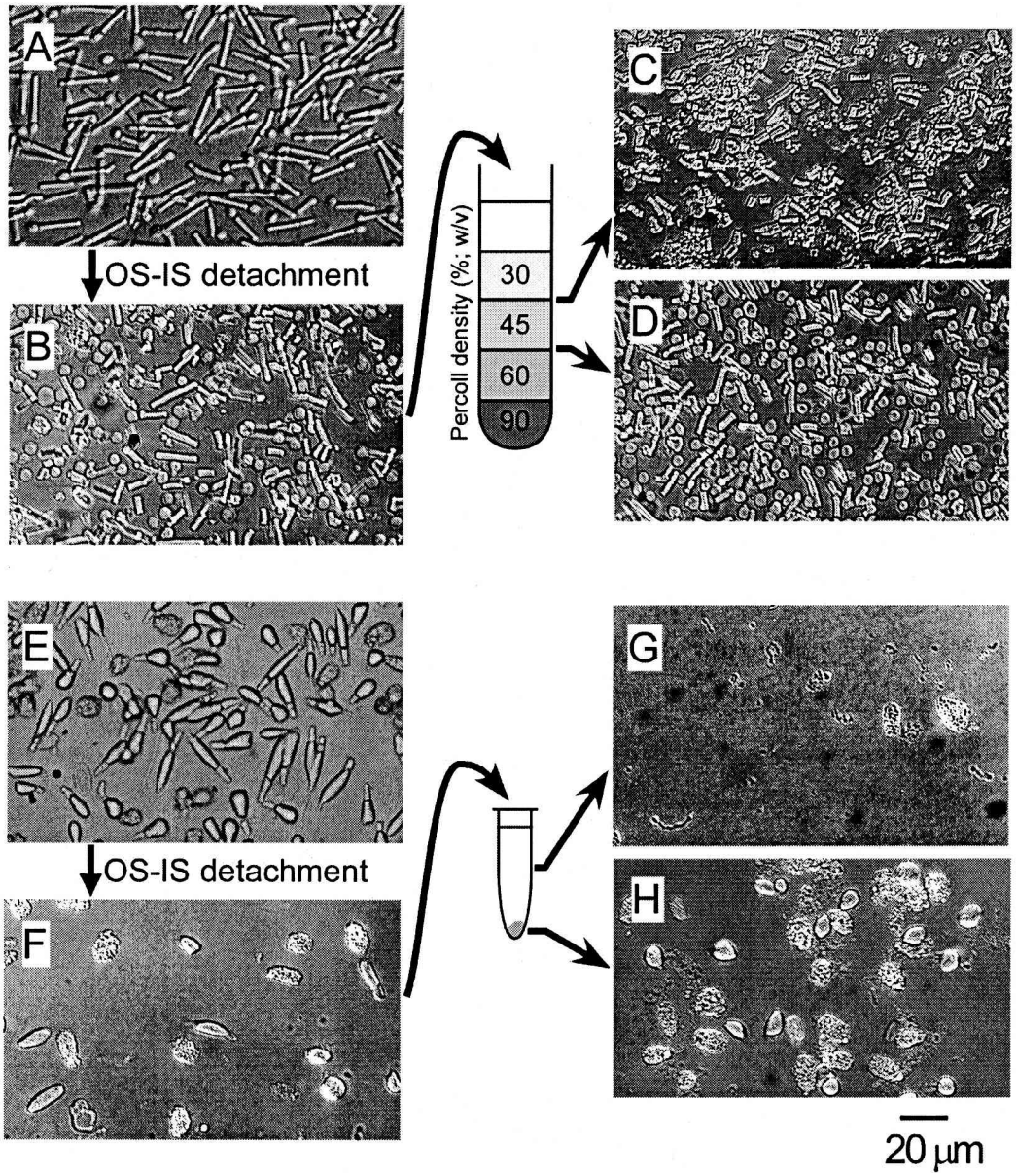

Figure 8. Preparation of OS- and IS-rich samples from purified rods and cones. (A) Purified rods. (B) Rods after passage through a 27-gauge needle. (C) ROS-rich fraction. (D) RIS-rich fraction. Spherical bodies in (B) and (D) would be the inner segments. (E) Purified cones. (F) Cones after passage through a 27-gauge needle. (G) COS-rich fraction. (H) CIS-rich fraction. Cone outer segments are not visibly identified in (F) and (G), but cone pigments are detected in these preparations spectrophotometrically.

To estimate the content of OS and IS in the OS- and IS-rich preparations, I quantified the amount of visual pigment as a marker of the OS, and the activity of mitochondrial succinate dehydrogenase (SDH) (Figure 9A), a quantitative marker of the IS. They were measured under a constant amount of visual pigment (Figure 9B and 9D). Most of my purified rods and cones retained both the OS and the IS, and the ratio of the SDH activity to the amount of visual pigment in the purified rods or cones was taken to be the index showing that the IS/OS ratio is 1.0 (Figure 9C and 9E).

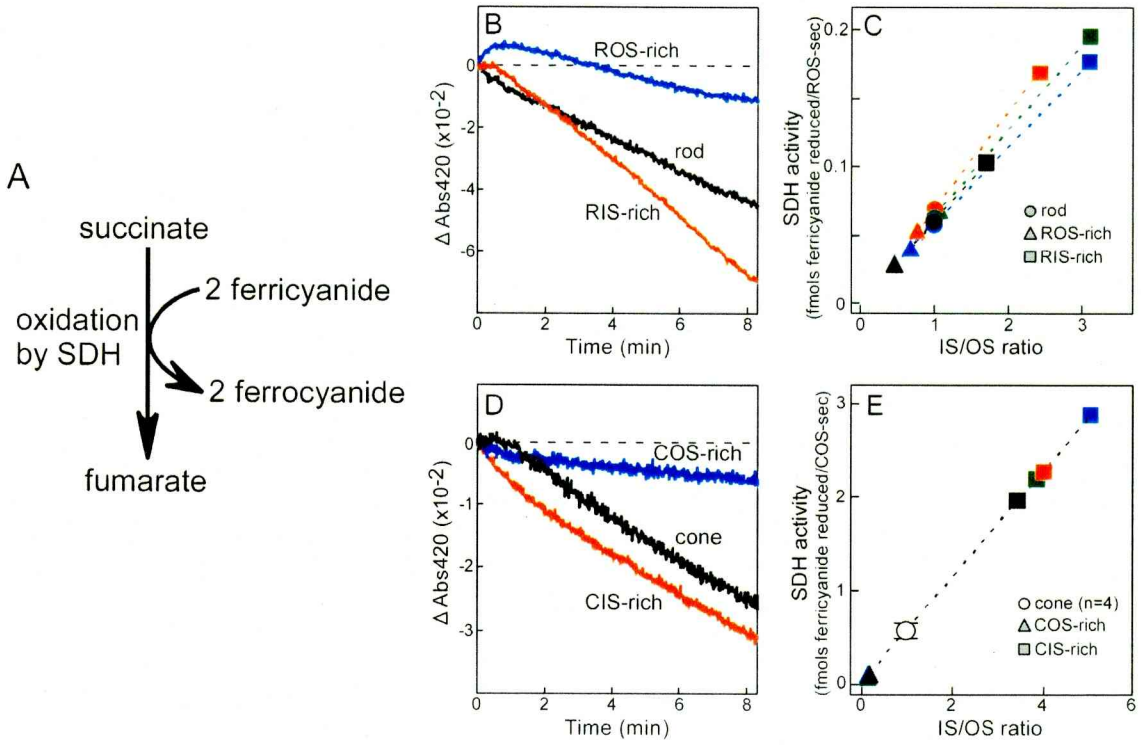

Figure 9. SDH activity in rod and cone preparations. (A) SDH reaction schema. Oxidation of succinate to fumarate is accompanied with reduction of ferricyanide to ferrocyanide. (B) SDH activity measured in rod preparations. Absorbance decrease at 420 nm due to reduction of ferricyanide by SDH was measured in the lysates of ROS-rich, purified rod (rod) and RIS-rich preparations all containing constant 100 pmols of rod pigment. The steeper decline of the absorbance in RIS indicates that the SDH activity, and therefore, the content of IS is higher in this preparation under the constant amount of rod pigment, and thus, the OS. Because a rod in the purified rod preparation possesses both the OS and the IS, the SDH activity in "rod" preparation was taken to be an indication that the ratio of IS/OS is 1.0. Symbols filled with the same color indicate the results obtained from the same starting purified rods. (C) Summary of the results. The SDH activities were plotted against the relative content of IS to that of OS. (D) Similar as in (A) except that the COS-rich, purified cone and CIS-rich preparations contained 3.0, 3.0 and 0.75 pmols of visual pigment, respectively. (E) Similar as in (C) except that the SDH activity in purified cones was taken to be an indication that the ratio of IS/OS is 1.0.

All of the rod samples, namely purified rods, rod OS (ROS)- and rod IS (RIS)-rich preparations, contained small amount of cones. To correct the contribution of cones, the amount of the cone OS (COS) and the cone IS (CIS) in rod preparations were determined (Figure 10). Carp retina contains four types of cone visual pigment. Among them, the content of the red-sensitive pigment is most abundant. The COS contamination was estimated on the bases of the amount of red pigment in rod preparations and the relative

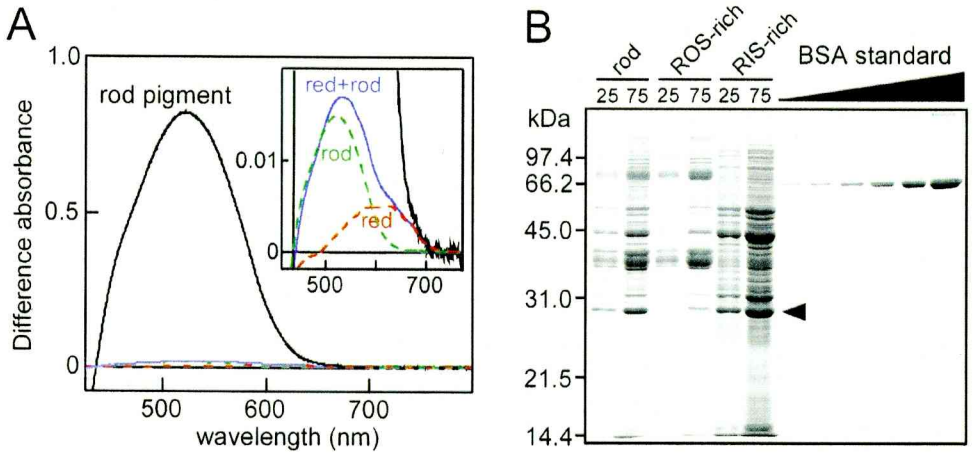

C

sample	cone contamination (% ratio of OS or IS;mean ± SD) COS (cone pigment)	CIS (ES1 protein)
purified rod	1.3 ± 1.0	1.5 ± 0.7
ROS-rich	not detected	0.46 ± 0.34
RIS-rich	not detected	2.9 ± 1.7

Figure 10. Cone contamination in rod preparations. (A) Estimation of the amount of contaminated cone pigment in a purified rod preparation. In one portion of the sample, rod pigment in the purified rods was quantified by the difference of the absorption spectral before and after the bleach with >460 nm light (rod pigment, black curve in A). In the other portion, the sample was illuminated with >680nm light extensively to bleach all of the red pigment. The difference in the absorption spectrum before and after the illumination was measured (curve shown in purple in insect). This curve consists of the spectrum of rod pigment (green dotted curve) and that of the red pigment (red dotted curve). Using the template of the absorption spectrum of red pigment, the amount of red pigment was quantified. (B) Estimation of the CIS contamination. The purified rod, ROS-rich and RIS-rich preparations were applied to an SDS-PAGE. Each number shows the pmols of visual pigment applied to each lane. The protein bands of ES1 (arrowhead) were quantified by comparing the protein band density of BSA standards. (C) Summary of the cone (COS and CIS) contamination in the rod preparations. From the calculations shown in (A) and (B), the content of cone contamination were determined (n=4-6).

content of the red pigment among the cone visual pigment (50% in this study). The amount of red pigment was quantified by the partial bleach method (Figure 10A) as described previously (Tachibanaki et al., 2001). The CIS contamination was evaluated from the amount of ES1 protein, a marker of the CIS (Chang and Gilbert, 1997). The content of ES1 in each rod preparation was quantified (Figure 10B) and the contamination was calculated on the basis of the content of ES1 in each cone (3.3 ± 1.0 fmols/cone, n=6). ES1 is a soluble protein and should be lost from the contaminated CIS during preparation of the ROS- and RIS-rich samples. From a measurement using purified rods and cones, I found that 35.1 ± 21.1 % (n=4) of ES1 was lost during this procedure and this loss was taken into consideration when necessary.

The summarized result of the contamination of cones in purified rod, ROS-rich and RIS-rich preparations is shown in Figure 10C. In my purified rod preparation, the COS contamination was 1.3 ± 1.0% (n=10) and the CIS contamination was 1.5 ± 0.7% (n=6). In ROS- and RIS-rich samples, the COS contamination was negligible, but the CIS contamination was 0.46 ± 0.34% (n=4) in the ROS-rich samples and 2.9 ± 1.7% (n=4) in the RIS-rich samples. All of the above contaminations were corrected in the estimation of the distribution of the RDH activities in the ROS and the RIS.

I measured the RDH activities in the OS-rich and the IS-rich preparations of rods and cones (Figure 11). In this figure, I plotted the RDH activity as a function of the content of the IS relative to that of the OS in rod (Figure 11A) and cone preparations (Figure 11C).

As can be seen in Figure 11A, in the rod preparations, the activity increased significantly as the content of the IS increased, which indicated that the RDH activity is present in the IS of a rod. From the ratio of IS/OS, I calculated the RDH activities in the ROS and in the RIS. The estimated RDH activity was 0.64 ± 0.11 amols atROL/ROS-sec, and 0.80 ± 0.11 amols atROL/RIS-sec (Figure 11B). In rods, the estimated activities in the OS and in the IS were nearly equal. In the ROS, the activity was equivalent to 2.4 ± 0.3 x 10^{-3} molecules of atROL formed/pigment-sec (molecules atROL/pigment-sec) (Figure 11E).

Similarly, I measured the RDH activities in the cone OS (COS)-rich and the cone IS (CIS)-rich preparations. The overall reducing activity was higher in the cone preparations (Figure 11C) than in the rod preparations (Figure 11A) (note the difference in the unit of the

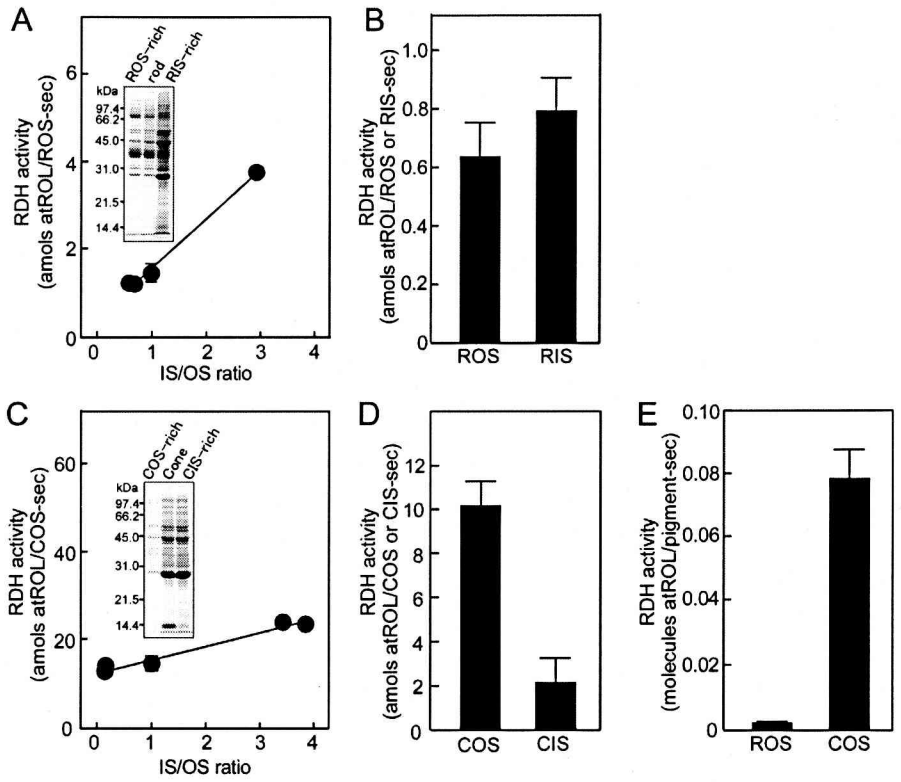

Figure 11. RDH activities in the OS and the IS of rods and cones. (A) RDH activities were measured in the ROS- and the RIS-rich preparations, and plotted against the content of the IS. The OS and the IS ratio in our purified rods was taken to be 1.0 (see text). The content of the RIS was estimated as described in Experimental Procedures. (inset) SDS-PAGE patterns of the ROS-rich preparation, purified rods (rod) and the RIS-rich preparation. Note the difference of the protein expression patterns among the three preparations. (B) Estimated RDH activities in the ROS and in the RIS. The RDH activities in the ROS and in the RIS were calculated from the results of the RDH activities measured in various contents of the IS shown in (A) (n=3). (C) RDH activities in the COS-rich and the CIS-rich preparations were similarly determined as in (A). (inset) SDS-PAGE patterns of the COS-rich preparation, purified cones (Cone) and CIS-rich preparation. (D) RDH activities in the COS and in the CIS were estimated from the result shown in (C) (n=4). (E) RDH activities in the OS in rods and cones. From the results shown in (B) and (D), the RDH activities in the ROS and the COS are expressed in the unit of per visual pigment.

ordinate between Figure 11A and 11C) in agreement with the result shown in Figure 6. The notable point was that, in contrast to the result obtained in rod preparations (Figure 11A), the activity only slightly increased as the content of CIS increased. The result indicated that most of the RDH activity is present in the OS in cones. The estimated reduction activity was 10.2 ± 1.1 amols atROL/COS-sec, and 2.2 ± 1.1 amols atROL/CIS-sec (Figure 11D). In the COS, the activity was equivalent to 7.9 ± 0.9 x 10^{-2} molecules atROL/pigment-sec (Figure 11E).

From the estimated RDH activities in the ROS and the COS, the all-*trans* retinal reducing activity per unit volume of the OS was found to be 33 times ($7.9 \times 10^{-2} / 2.4 \times 10^{-3}$) higher in cones than in rods, which suggested that the reduction of all-*trans* retinal is much faster in cones (Figure 11E).

Three RDH Subtypes, RDH8, RDH8L2 and RDH13, are the Major RDH Subtypes Expressed in the Carp Retina

There are potentially two possible mechanisms that explain the higher RDH activity in cones. One is that the same subtype of RDH is expressed in rods and cones and that the expression level is much higher in cones. The other is that the RDH subtype(s) expressed in cones is different from that in rods and that the cone subtype(s) shows much higher activity than the rod subtype(s).

To identify RDH subtypes in rods and cones, I first isolated carp retinal cDNA fragments encoding RDH genes. It has been reported that RDH subtypes expressed in vertebrate photoreceptor cells are RDH8, RDH11, RDH12, RDH13, RDH14, and short chain dehydrogenase/reductase (retSDR1) (Haeseleer et al., 1998; Rattner et al., 2000; Haeseleer et al., 2002). On the basis of the amino acid sequences of these RDHs, I synthesized oligonucleotide degenerate primers and used them to search for the cDNA fragments of carp homologues of the vertebrate photoreceptor RDHs. I obtained eleven partial carp RDH genes; three RDH8, three RDH12, two RDH13, one RDH14, and two retSDR1 homologous genes from a carp retinal cDNA (Figure 12A). Additionally, a carp cDNA fragment of RDH5 homologous gene was isolated from the RPE as a marker of the RPE.

To determine the relative abundance of these mRNAs, semi-quantitative RT-PCR analysis was performed using primers against these twelve RDHs. Although RDH8 and RDH13 have been reported to be expressed mainly in photoreceptor cells in primate (Rattner et al., 2000; Haeseleer et al., 2002), I found that RDH8, RDH8L2 and RDH13 were expressed at higher levels in the carp retina, and that RDH5 and retSDR1 were predominantly expressed in the RPE (Figure 12B). Other genes including those of RDH12 and RDH14 were not detected significantly. Assuming that the relative abundance of an

mRNA reflects that of the corresponding protein, I concluded that the three RDH proteins, RDH8, RDH8L2 and RDH13, are expressed at much higher levels than other RDHs in the carp retina. Thus, carp retinal cDNA library was screened, and the full-length cDNA sequences of these three RDH genes were obtained. These sequences were used for the phylogenetical analysis (Figure 12A), and for the expression of recombinant proteins (see below).

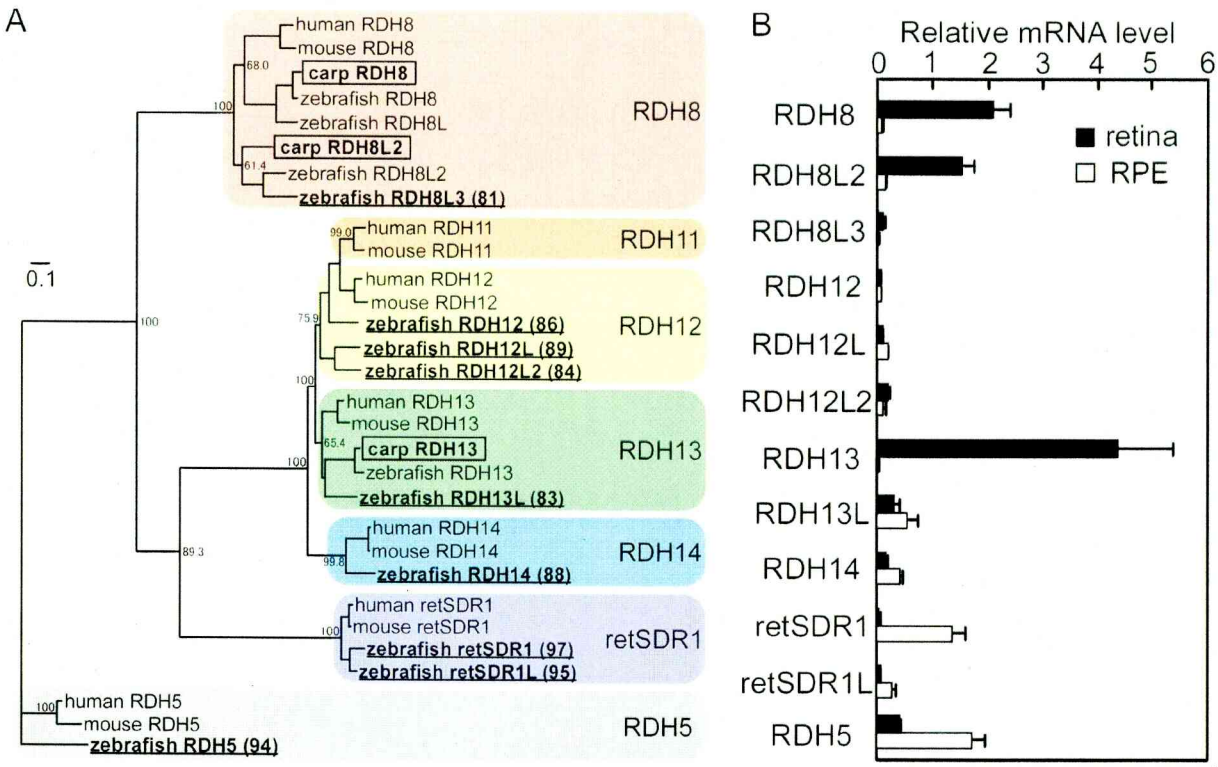

Figure 12. Subtypes of RDH in the carp retina. (A) Molecular phylogenetic tree of vertebrate RDH genes. Bootstrap probabilities are shown at the nodes as the percentages from 1000 rewriting. The scale bar represents 0.1 amino acid substitutions per position in the sequences. Each number in parentheses shows the percentage of identity of the amino acid sequence of a carp RDH gene fragment to a corresponding zebrafish RDH gene. RDH genes shown in boxes are those in which full length of the amino acid sequences were determined. (B) Relative mRNA expression levels of RDHs in the carp retina and the RPE. The mRNA expression levels of RDHs relative to that of short chain dehydrogenase/reductase (retSDR1) in the retina were determined with a semi-quantitative RT-PCR reaction. To compare the levels between the retina and the RPE, the expression levels were normalized by the amount of 18S ribosomal RNA in each tissue. Error bars show standard deviations determined in three independent preparations (two determinations in each preparation).

Expression levels and Distribution of RDH8, RDH8L2 and RDH13 in Rods and Cones

To determine which subtype of RDH is responsible for the RDH activities in the OS and in the IS, first I quantified the amount of each subtype in the OS and the IS of rods and cones. For this, I raised specific antiserum against each subtype (Figure 13A and 13B). It was found with immunoblots that all of the three subtypes are present in the membrane fraction of rods and cones (Figure 13C). By using purified rods and cones, the contents of the RDHs in the preparations were quantified by immunoblot analyses with known amounts of RDHs as standards (Figure 13D and 13E, but in Figure 13E, only the result of RDH8 in purified rods is shown as an example). The summarized result of the content of RDH8, RDH8L2 and RDH13 in rods and cones is shown in Figure 13F, where the content is expressed in the unit of per rod or cone. It was found that all of the these subtypes of RDH are expressed much more abundantly in cones.

Furthermore, the relative distributions of the RDHs in the OS and the IS of rods and cones were determined. In this determination, by using the OS- and the IS-rich samples together with purified rods and cones as used in the study shown in Figure 11, the contents of the RDHs in these preparations were quantified (Figure 14A and 14C; in each figure, only the quantification of RDH8 is shown in the lower panel). Based on these relative distributions (Figure 14B and 14D) and the total contents of the three RDHs (Figure 13F), the total number of each RDH molecule in the OS and the IS of rods and cones was calculated.

The summarized result of the content of RDH8, RDH8L2 and RDH13 in the OS and the IS of rods and cones is shown in Figure 14E, where the content is expressed in the unit of per OS or IS. It was found that (i) all the RDHs were 5-40 times more abundant in cones than in rods, (ii) in both rods and cones, RDH8 localizes almost exclusively in the OS, (iii) among RDHs, RDH8L2 was the most abundant RDH in both rods and cones, and (iv) RDH8L2 and RDH13 localize predominantly in the IS. The localization of RDH8 and RDH13 is similar to that previously reported in primates (Rattner et al., 2000; Haeseleer et al., 2002). Carp RDH8L2 is one of the RDH8 homologs, but localizes in the IS unlike other vertebrate RDH8s.

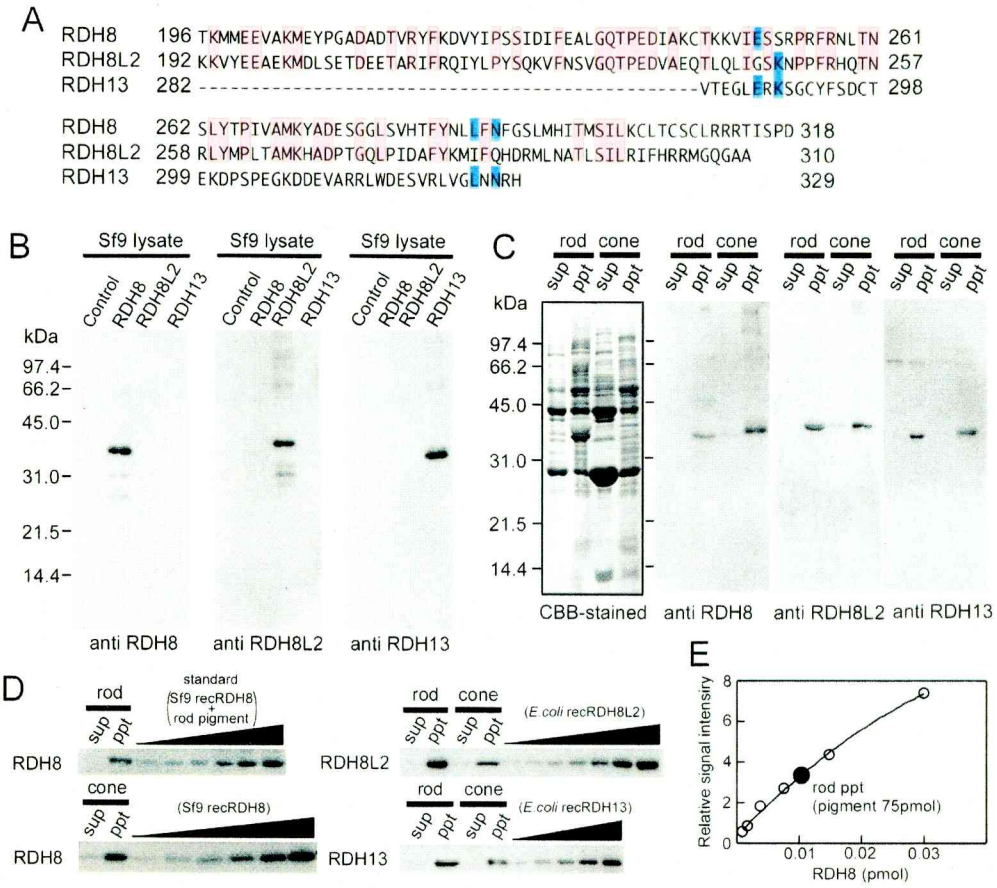

Figure 13. Relative distribution of RDH8, RDH8L2 and RDH13 in the OS and the IS of rods and cones. (A) RDH partial peptides used for immunization. Anti-RDH8, RDH8L2 and RDH13 antisera were raised against each purified GST-fused peptide in mice. (B) Specificity of antiserum used. Antiserum against each RDH was raised, and its specificity was checked by recombinant RDH expressed in Sf9 cells. Eighty fmols of each RDH in Sf9 cells were applied in each lane. (C) SDS-PAGE pattern (left panel) and immunoblots of purified rods and cones (the rest of three panels). Rods containing 400 pmols of visual pigment or cones containing 20 pmols of visual pigment were homogenized and centrifuged. Both the precipitated membrane fraction (ppt) and the supernatant soluble fraction (sup) were applied to SDS-PAGE (left). Rod and cone proteins were probed with the antiserum raised against RDH8 (middle left), RDH8L2 (middle right) and RDH13 (right). (D) Estimation of the contents of the three RDH subtypes in rods and cones. The immunoblot signals of the three RDH subtypes in rods and cones and the signal of recombinant RDHs (recRDHs) as standards (see Experimental Procedures) were detected. (E) The calibration curve of each RDH subtype was obtained from the signals of standard recombinant proteins shown in (D). The signals from standards (open circles) and the eye-fitted calibration curve for RDH8 are shown as an example. The content in the sup and the ppt fraction was quantified by using the calibration curve (filled circle). Signal of RDH8 in the sup fraction was not detected. (F) Summary of the expression levels of RDH8, RDH8L2 and RDH13 in rods and cones. From the quantification shown in (D) and (E), the expression levels of three major RDHs were determined (n=5-12).

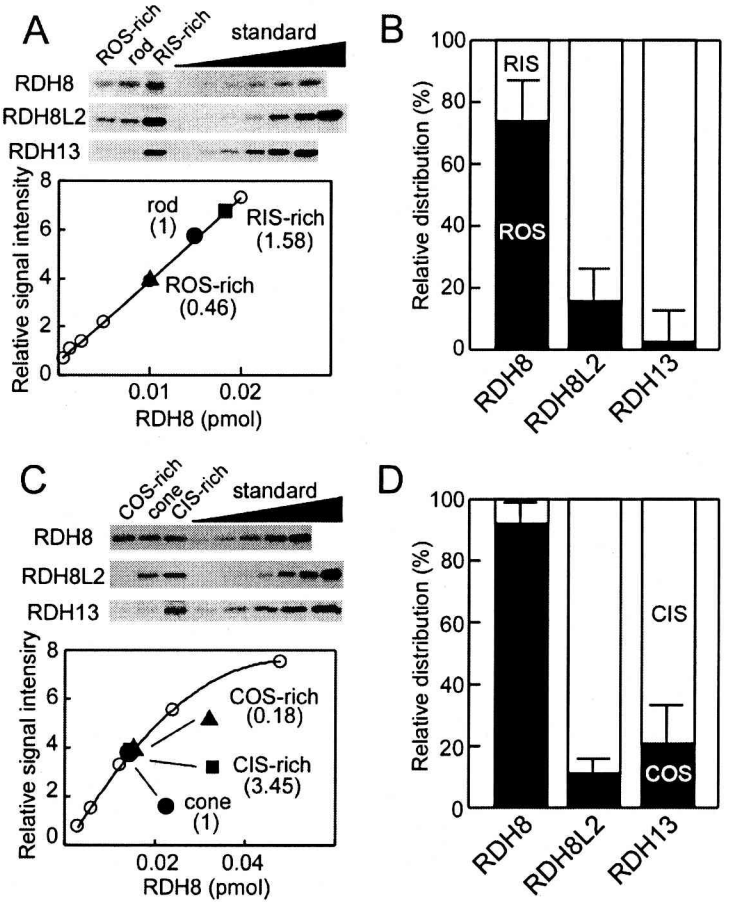

E

Number of RDH molecules / OS or IS (x10^4;mean ± SD)

		RDH8	RDH8L2	RDH13
rod	OS	1.4 ± 0.2	3.9 ± 2.6	0.1 ± 0.2
	IS	0.5 ± 0.2	20.7 ± 2.6	2.2 ± 0.2
cone	OS	29.2 ± 2.2	20.0 ± 22.7	4.3 ± 2.5
	IS	2.5 ± 2.2	159.2 ± 22.7	16.2 ± 2.5

Figure 14. Distribution of RDH8, RDH8L2 and RDH13 in the OS and the IS of rods and cones. (A) Determination of expression levels of RDHs in the ROS and the RIS. (Upper) The ROS-rich, purified rod and the RIS-rich preparation all containing 75 pmols of visual pigment, together with their recombinant standard proteins of known amounts were immunoblotted. (Lower) From the calibration curve obtained from the standard proteins, the amounts of RDH8 in the OS-rich, purified rod and the IS-rich preparation were determined. In this example, the content of the IS to the OS is shown in the parentheses. (B) Relative distribution of RDH8, RDH8L2 and RDH13 in the OS and the IS of rods (n=4). (C) Similar as in (A) except that the cone OS-rich, purified cone and the cone IS-rich preparation all containing 5 pmols of visual pigment were used. (D) Relative distribution of RDH8, RDH8L2 and RDH13 in the OS and the IS of cones (n=4). (E) Summary of the expression levels of RDH8, RDH8L2 and RDH13 in the OS and the IS of rods and cones. From the contents shown in (Figure 13F) and the relative distributions shown in (B) and (D), the expression levels of three major RDHs were determined (n=4).

RDH8 Contributes to the Highly Efficient All-*trans* Retinal Reduction in the Cone Outer Segment

As shown, all the three subtypes of RDHs (RDH8, RDH8L2, and RDH13) are expressed in rods and cones. The specific activities of these RDHs were measured by using recombinant RDH proteins expressed in HEK293 cells (Figure 15). The expression of RDH in HEK293 cells was confirmed by immunoblot analysis with specific antiserum (Figure 15A). Recombinant RDHs in the membrane fraction were used for the assay, and their contents were measured by immunoblot analysis. The specific activities of RDH8, RDH8L2 and RDH13, thus, obtained were 27.8 ± 10.1, 1.9 ± 0.9, and 1.5 ± 0.3 molecules of atROL formed/RDH molecule-sec, respectively (Figure 15B). The specific activity of RDH8 was >10 times higher than those of the others. The RDH activity was not detected in control HEK293 cells transfected with the empty vector.

Because I now know both the specific activity of each single RDH molecule (Figure 15B) and the number of each RDH molecule expressed in the OS and the IS of rods and cones (Figure 14E), I can simply calculate the total RDH activities in the OS and the IS of rods and cones (Figure 15C and 15D). The calculated results (colored bars in Figure 15C and 15D) are consistent with the RDH activities determined in the OS- and the IS-rich preparations in Figure 11B and 11D (re-drawn as black bars in Figure 15C and 15D), and showed that the activity in the OS is predominantly due to RDH8 (red area), and that the activity in the IS is mainly due to RDH8L2 (white area) in both rods and cones.

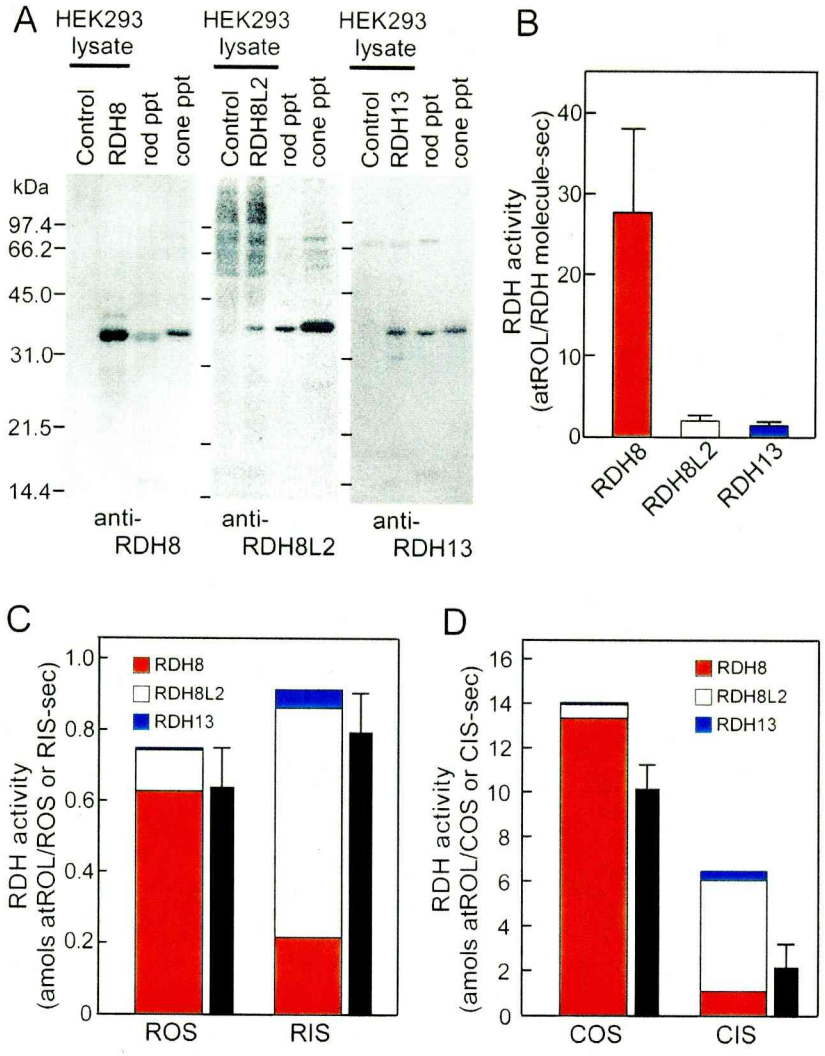

Figure 15. Specific activities of RDH8, RDH8L2 and RDH13, and their contribution to the RDH activities in the OS and the IS of rods and cones. (A) Immunoblots of HEK293 cells expressing the recombinant RDHs. HEK293 cells transfected with an empty vector (Control in each panel), vectors expressing RDH8 (Left), RDH8L2 (Middle), or RDH13 (Right), and the rod or cone membrane fraction (rod ppt and cone ppt, respectively, in each panel) were electrophoresed and detected with anti-RDH8 (Left), anti-RDH8L2 (Middle) and anti-RDH13 (Right) antiserum. (B) Specific RDH activities of recombinant RDH8, RDH8L2 and RDH13 expressed in HEK293 cells. Error bars show standard deviations (n=3-6). (C, D) RDH activities in the OS and the IS of rods (C) and cones (D) calculated from the specific activity (B) and the distribution (Figure 14E) of each RDH (colored bars). Black bars show the RDH activities determined in the OS- and the IS-rich preparations in Figure 11B and 11D.

11-*cis* Retinal is synthesized from 11-*cis* Retinol with a Retinal-Retinol Redox Coupling

It is known that visual pigments are regenerated after addition of 11-*cis* retinol in

isolated cones, but not in rods (Jones et al., 1989). It suggests that cones have a mechanism to convert 11-*cis* retinol to 11-*cis* retinal. It has been reported that 11-*cis* retinol is converted to 11-*cis* retinal in the presence of $NADP^+$ in a cone-dominant retina. This result suggests that $NADP^+$-dependent 11-*cis* retinol dehydrogenase is present in cones (Mata et al., 2002). This 11-*cis* retinol conversion in cones is thought to be necessary for a cone-specific visual cycle that should support highly efficient pigment regeneration in cones. However, as shown in Figure 7B, at least in our purified carp cones, production of 11-*cis* retinal from 11-*cis* retinol was not so effective.

Oxidation of retinol to retinal by RDHs is always coupled with reduction of a cofactor, $NADP^+$ (Figure 16 upper). It is possible that, instead of $NADP^+$, other chemicals, for example, all-*trans* retinal could substitute the role of $NADP^+$ (Figure 16 lower). To test this possibility, I measured the conversion of 11-*cis* retinol to 11-*cis* retinal in the rod and cone lysates in the presence of all-*trans* retinal but in the absence of $NADP^+$.

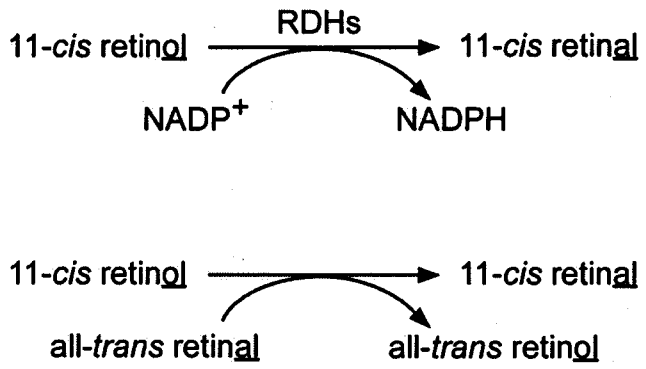

Figure 16. Reaction scheme of oxidation of 11-*cis* retinol to 11-*cis* retinal. (upper) Oxidation of 11-*cis* retinol to 11-*cis* retinal is accompanied by reduction of $NADP^+$ to NADPH. RDH reaction requires $NADP^+$ as a cofactor. (lower) Hypothesized oxidation of 11-*cis* retinol is accompanied by reduction of all-*trans* retinal to all-*trans* retinol. Oxidation of alcohol requires reduction of aldehyde.

In Figure 17, the reaction products were analyzed by HPLC. It was evident that after 10 min incubation in the cone lysate (lower panel in Figure 17B), two peaks of 11-*cis* retinal (red arrowhead) and two peaks of 13-*cis* retinal (open arrowhead) were newly formed. Further, all-*trans* retinol (blue arrowhead) was additionally formed. Because retinals were detected in the form of oximes, there are two *syn-* (s) and *anti-* (a) stereo-isomers. Similar

studies were performed by using rod lysate (Figure 17C), but 11-*cis* retinal was not produced. These results showed that 11-*cis* retinal was produced specifically in cones. Therefore, I examined this reaction in detail.

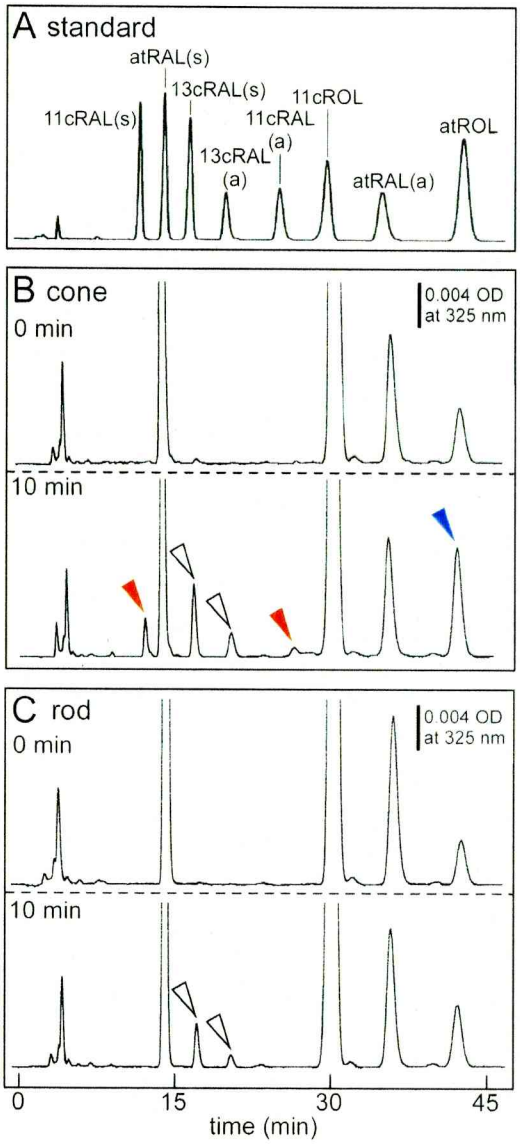

Figure 17. HPLC analysis of retinoids in cones and rods in the presence of both 11-*cis* retinol and all-*trans* retinal. (A) A representative HPLC chromatogram of retinal-oxime and retinol standards: 11cRAL(s/a), *syn*-/*anti*-11-*cis* retinal oxime; atRAL(s/a), *syn*-/*anti*-all-*trans* retinal oxime; 13cRAL(s/a), *syn*-/*anti*-13-*cis* retinal oxime; 11cROL, 11-*cis* retinol; atROL, all-*trans* retinol. (B) A representative HPLC chromatogram of retinoids extracted from cone lysate incubated with 11-*cis* retinol and all-*trans* retinal for 0 min (upper) and 10 min (lower). Note that the peaks of 11-*cis* retinal oximes (red arrowhead), 13-*cis* retinal oximes (white arrowhead) and all-*trans* retinol (blue arrowhead) are additionally detected in the lower panel. (C) Similar as in (A) except that the rod lysate was used. Note that the peaks of 13-*cis* retinal oximes (open arrowhead) are additionally detected in the lower panel.

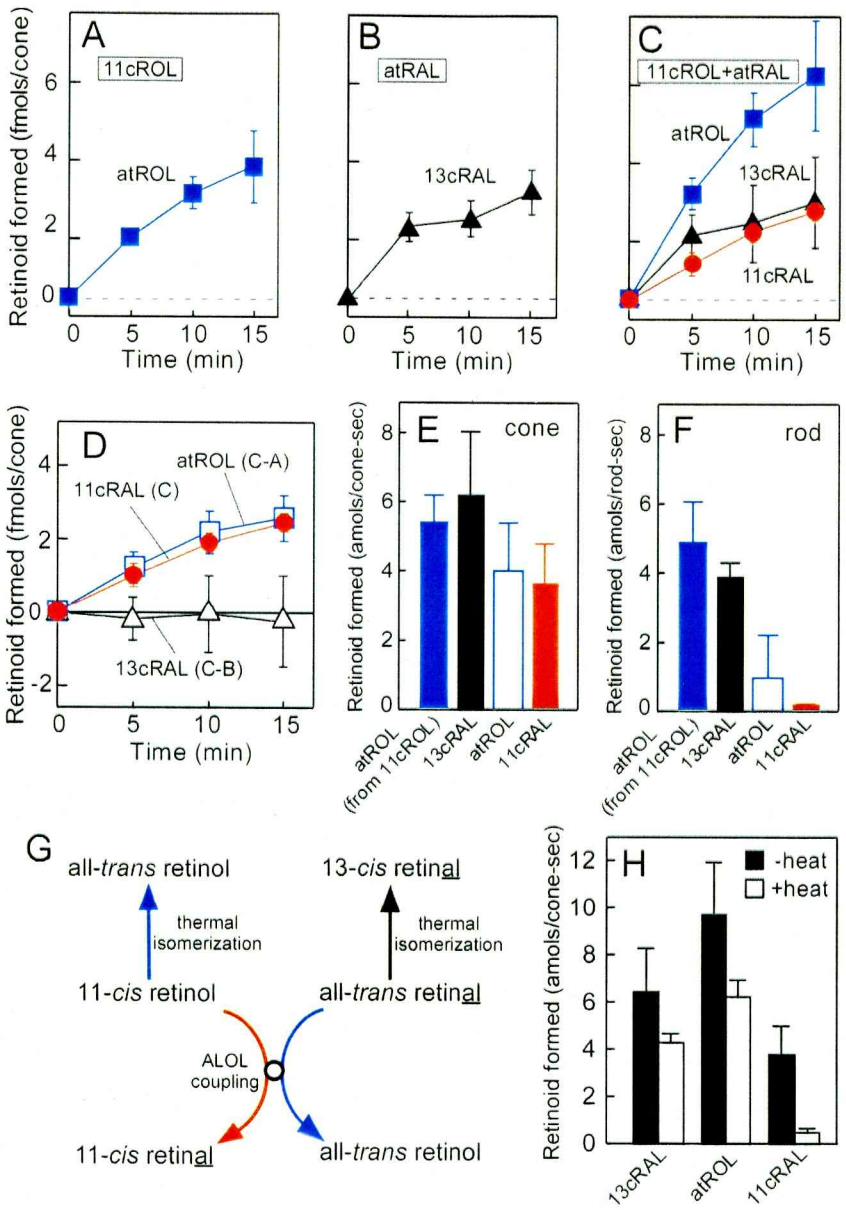

Figure 18. Formation of 11-*cis* retinal from 11-*cis* retinol in the absence of NADP$^+$ in cones. (A) Time course of thermal isomerization of 11-*cis* retinol (11cROL) to all-*trans* retinol (atROL) in the cone lysate (n=5). (B) Time course of thermal isomerization of all-*trans* retinal (atRAL) to 13-*cis* retinal (13cRAL) in the cone lysate (n=3). (C) Time course of retinoids formation in the cone lysate in the presence of both 11-*cis* retinol and all-*trans* retinal (n=5). (D) Net effect of the coexistence of 11-*cis* retinol and all-*trans* retinal. The amounts of thermally isomerized products in (A) and (B) were subtracted from those in (C) to calculate the extra formation of 11-*cis* retinal, all-*trans* retinol and 13-*cis* retinal. Note that 11-*cis* retinal and all-*trans* retinol were formed with a 1:1 stoichiometry. (E, F) Initial rates of retinoid formation in the presence of both 11-*cis* retinol and all-*trans* retinal in the cone lysate (E) and the rod lysate (F). The rates were determined from the amounts of retinoids formed at 5 min after the initiation of the reaction (n=5 for cones and n=3 for rods). (G) Reaction scheme in the cone lysate with addition of 11-*cis* retinol and all-*trans* retinal. See text for details. (H) Effect of heat treatment on the formation of 11-*cis* retinal from 11-*cis* retinol in the presence of all-*trans* retinal. The amount of formed retinoid in the presence of both 11-*cis* retinol and all-*trans* retinal was determined in the cone lysate that was treated with or without heat (+heat (65 °C for 5 min) and -heat) (n=3 for +heat, and n=5 for -heat).

It has been shown that retinoids are thermally isomerized significantly in the presence of rod membranes (Groenendijk et al., 1980; Shimizu et al., 1998). I confirmed it in the presence of the cone lysate: 11-*cis* retinol was isomerized almost exclusively to all-*trans* retinol (Figure 18A), and all-*trans* retinal was also exclusively isomerized to 13-*cis* retinal (Figure 18B). In these measurements, 11-*cis* forms were not detected. When 11-*cis* retinol and all-*trans* retinal were added simultaneously to the cone lysate, 11-*cis* retinal was additionally formed (Figure 18C, red line). In addition, all-*trans* retinol was also formed in a corresponding amount (compare blue lines in Figure 18A and 18C). The net effect of the presence of both 11-*cis* retinol and all-*trans* retinal was obtained by subtraction of the control values shown in Figure 18A and 18B from the values shown in Figure 18C, which is shown in Figure 16D. It was evident that 11-*cis* retinal and all-*trans* retinol were newly produced in the presence of 11-*cis* retinol and all-*trans* retinal. The stoichiometry of the formation of 11-*cis* retinal and all-*trans* retinol was close to 1:1 (compare white bar and red bar in Figure 18E). Figure 18G shows all of reactions of retinoids in cone lysate with addition of 11-*cis* retinol and all-*trans* retinal. This result strongly suggests that, in cones, 11-*cis* retinol can be oxidized to 11-*cis* retinal accompanied by the reduction of all-*trans* retinal to all-*trans* retinol. This retinal-retinol redox coupling reaction (ALOL coupling) was not observed in the rod lysate (Figure 18F). The cone lysate treated with heat showed little this activity (Figure 18H), which suggested that the ALOL coupling is an enzymatic reaction.

To examine physiological relevance of this coupling, I examined whether all-*trans* retinal produced by light can participate in the ALOL coupling when exogenous 11-*cis* retinol is supplied (Figure 19A). The exogenous 11-*cis* retinol (A1 11-*cis* retinol) and the endogenous all-*trans* 3,4-didehydroretinal (A2 all-*trans* retinal; the chromophore of visual pigment in carp is vitamin A2-based 11-*cis* retinal) were used for this visual pigment regeneration assay (Figure 19A). The endogenous A2 all-*trans* retinal was formed by illumination of light. First, I measured the absorption spectrum of red cone pigment in a carp membrane preparation (Figure 19B, grey dotted line) as described (Tachibanaki et al., 2001), and using the bleached cone membranes, I observed the visual pigment regeneration as a control by adding excess amount of A1 11-*cis* retinal as a control (blue line). The shift of the peak was due to the difference of the chromophore type, A2 11-*cis* retinal (λ_{max}= ~620nm) or A1 11-*cis* retinal (λ_{max}=~570nm).

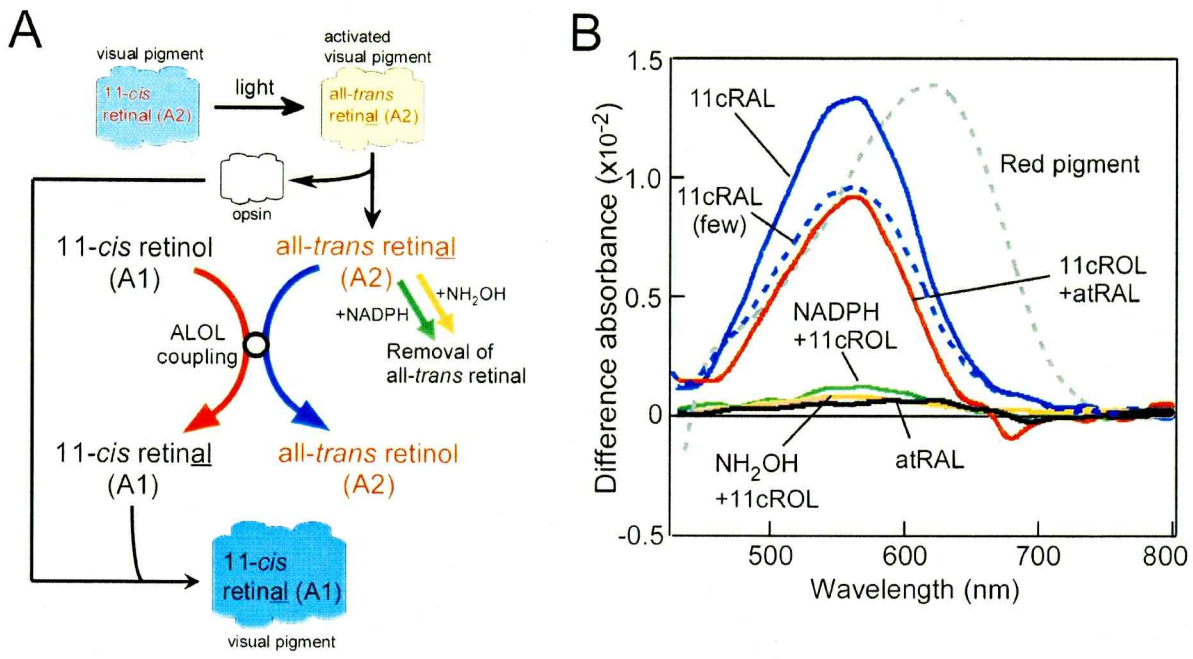

Figure 19. Visual pigment regeneration by ALOL coupling reaction. (A) Reaction scheme in the cone lysate under the condition of visual pigment regeneration assay. See text for details. (B) Difference absorption spectra of red cone pigment regenerated under the various conditions (see text). The spectra were measured by the partial bleach method (see Experimental Procedures).

The native cone membranes having A2 11-*cis* retinal were illuminated, and as a consequence, A2 all-*trans* retinal should have been formed and released from the bleached pigment. When A1 11-*cis* retinol was added to these membranes, as expected, visual pigment was regenerated (red line). Although the regeneration was about 70% of the control measurement (blue line), it was evident that 11-*cis* retinal was produced most probably by the ALOL coupling with the endogenous all-*trans* retinal released from the bleached pigment. Similar percentage of pigment regeneration was observed when I added 11-*cis* retinal of the amount calculated to be the same to that of endogenously formed all-*trans* retinal (blue dotted line). Pigment regeneration was not observed without addition of 11-*cis* retinol (black line), with addition of 11-*cis* retinol after removal of all-*trans* retinal by NH_2OH (orange line), or with addition of 11-*cis* retinol after all-*trans* retinal was converted to all-*trans* retinol by endogenous RDHs in the presence of NADPH (green line). This regeneration assay confirmed that the ALOL coupling is a potential mechanism that may play a crucial role in the cone visual cycle. Figure 20 summarizes the kinetic

parameters of the RDH reactions and the ALOL coupling reaction in rods and cones. The K_m value for all-*trans* retinal of the ALOL coupling in cones was several times larger than that of RDH reaction in cones, and the V_{max} was several times smaller in the coupling reaction.

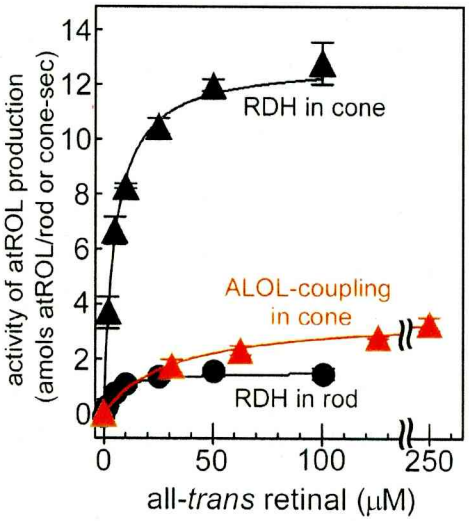

	Cell type	K_m (μM)	V_{max}*
RDH (NADPH)	rod	6.2 ± 2.2	2.1 ± 0.4
	cone	6.1 ± 2.2	14.3 ± 1.3
ALOL coupling (11-*cis* retinol)	rod	-	-
	cone	33.0 ± 8.8	3.5 ± 0.3

*amols of atROL/rod or cone-sec

Figure 20. Kinetics of the RDH and the ALOL coupling reaction in photoreceptors. (Left) All-*trans* retinal dose-dependence of the RDH activities in rods and cones (black) and the ALOL coupling activity in cones (red). (Right) Summary of the kinetic parameters of the RDH and the ALOL coupling reaction in rods and cones. The parameters were determined for the reduction of all-*trans* retinal to all-*trans* retinol (n=3). The RDH activities were measured at various concentrations of all-*trans* retinal with 200 μM NADPH (saturating concentration) and the activity of the ALOL coupling was measured at various concentrations of all-*trans* retinal with 250 μM 11-*cis* retinol (saturating concentration). The NADPH or 11-*cis* retinol shown in parentheses oxidized accompanied by reduction of all-*trans* retinal to all-*trans* retinol.

Discussion

In the present study, I showed that the RDH activity is ~30 times higher in the OS in cones than in rods (Figure 11). This higher activity in the cone OS is due to a higher expression level of RDH8, a highly potent RDH, in cones (Figures 14 and 15). In the IS, RHD8L2 is the major RDH in both rods and cones (Figures 14 and 15). I further demonstrated that there is a cone-specific mechanism that can oxidize 11-*cis* retinol to 11-*cis* retinal with a coupling reaction between reduction of all-*trans* retinal and oxidation of 11-*cis* retinol (ALOL coupling, Figure 18).

Physiological Relevance of the Measured RDH activity

In the legend to Figure 11E, I showed that the reducing activity of all-*trans* retinal is $2.4 \pm 0.3 \times 10^{-3}$ molecules atROL/pigment-sec in the ROS and $7.9 \pm 0.9 \times 10^{-2}$ molecules atROL/pigment-sec in COS, or 7.2 ± 0.9 μM atROL/sec in the ROS and 240 ± 30 μM atROL/sec in the COS assuming that the visual pigment concentration in the OS in both rods and cones is 3 mM (Harosi, 1975). The activity was 33 times higher in the COS than in the ROS. These values show that after 100% bleach of visual pigment molecules, a half of all-*trans* retinal is converted to its alcohol at about 5 min in the ROS and 8.5 sec in the COS. In living rods and cones, the formation of all-*trans* retinol after bleach was measured (Ala-Laurila et al., 2006). The times necessary for the half conversion of all-*trans* retinal to its alcohol, which were calculated from their results, were 6.4 min in the ROS and 16 sec in the COS. Although these are the values that were obtained in the overall reaction including both the decay of the bleaching intermediate of visual pigment and reduction of all-*trans* retinal, the results of our *in vitro* measurements of the RDH activity are consistent with those measured in living tiger salamander rods and cones. Because $NADP^+$ has an inhibitory effect on the reduction of all-*trans* retinal (Nicotra and Livrea, 1982) and is present in the amount of approximately 4 times excess than NADPH in monkey and rabbit ROS (Matschinsky, 1968), the slightly lower rate of the reduction of all-*trans* retinal in living cells may be due to the presence of $NADP^+$.

The RDH activities measured in the present study can be expressed in other ways:

based on the OS RDH activity, the production of all-*trans* retinal by light and its conversion to all-*trans* retinol is approximately balanced at the intensity of light bleaching 0.24% of pigment/sec in rods and that bleaching 7.9% of pigment/sec in cones. These intensities of light seem to be above the range where rods and cones normally operate. Therefore, the RDH activity in the OS seems to be high enough for both rods and cones to work under normal conditions.

I measured the maximal RDH activity in purified carp rods and cones. One question was whether NADPH necessary for the reduction of all-*trans* retinal by RDHs is sufficiently present to exert the maximal RDH activity in a living cell. NADPH is produced in the OS mainly in the pathway of glucose metabolism (Hsu and Molday, 1994). It is thought that, in the OS, there is a pool of NADPH that may correspond about 10% of the visual pigment in the dark state (Ala-Laurila et al., 2006). After this pool is exhausted, the rate of the all-*trans* retinal reduction is limited by the rate of NADPH supply (Tsina et al., 2004).

The rate of NADPH production in the bovine ROS under optimal *in vitro* conditions is 40 nmols/min/mg of total ROS protein (Hsu and Molday, 1994). Assuming that a single bovine ROS contained approximately 16–20 nmols of rod pigment/mg of total ROS protein (Wald and Brown, 1953) and that the pigment concentration is 3 mM (Harosi, 1975), the rate of NADPH production is calculated to be 110 μM ((40 nmols/18 nmols/60 sec) x 3 mM) NADPH formed/sec. The reduction of one all-*trans* retinal molecule requires one NADPH molecule. Because our estimation of the maximal RDH activity was 7.2 ± 0.9 μM atROL formed/sec in the ROS (Figure 11, and see above), the rate of NADPH generation is sufficient to support the reduction of all-*trans* retinol in the ROS. The reducing activity of RDH in the COS (240 ± 30 μM atROL formed/sec; Figure 11) is 2 times higher than the NADPH supply rate determined in the ROS (110 μM NADPH formed/sec, see above). This result may suggest that NADPH supply is more efficient in the COS than in the ROS.

Possible Role of Each Subtype of RDH in Photoreceptors

I identified RDH8, RDH8L2 and RDH13 as major RDHs expressed in photoreceptors (Figure 12). RDH8 was predominantly expressed in the OS and RDH8L2 was expressed significantly in the OS but mainly in the IS in both rods and cones (Figure 14). RDH13 was

expressed mostly in the IS in both rods and cones (Figure 14). These site-specific expressions of these RDHs are probably related to their roles in rods and cones.

RDH8 accounted for > 80 % of the OS RDH activity (84% in the ROS, and 95% in the COS; Figure 15C and 15D), and therefore, it is the major RDH responsible for the reduction of all-*trans* retinal in the OS. However, genetical deletion of the RDH8 gene caused only a mild phenotype alteration of delayed dark adaptation (Maeda et al., 2005). No RDH8 mutations have yet been identified in patients with retinal diseases. It seems that the deletion of RDH8 could be compensated by overexpression of other RDHs.

RDH8L2 localized in the IS, and accounted for most of the RDH activity in the IS of rods and cones (Figure 15C and 15D). The total expression level was about 7 times higher in cones. However, because the IS volume is correspondingly larger in cones than in rods (my rough estimate of the ratio of the CIS volume to the RIS volume in my carp preparation was ~13; CIS/RIS=448/35 μm^3), the concentration of RDH8L2 in the IS could be similar between rods and cones. The K_m value for all-*trans* retinal of the RDH reaction was similar between RDH8 and RDH8L2 expressed in HEK293 cells (7.2 ± 0.8 and 5.0 ± 2.8 μM, respectively), but the specific activity of RDH8L2 was much lower than that of RDH8 (Figure 15B). This result strongly suggests that the physiologically relevant substrate of RDH8L2 may not be retinal. In the mammalian retina, RDH12 is abundant in the IS and accounts for 30% of the activity of all-*trans* retinal reduction in the eye (Haeseleer et al., 2002; Maeda et al., 2007). Interestingly, RDH12 shows reducing activity not only toward all-*trans* retinal but also toward medium-chain peroxidic aldehydes, such as nonanal, *trans*-2-nonenal and 4-hydroxynonenal (Belyaeva et al., 2005; Lee et al., 2008). These substrates are toxic to cells and lead to cell death for their ability to form lipid peroxidation products and *N*-retinylidene-*N*-retinylethanolamine (A2E), a major lipofuscin component (Eldred and Lasky, 1993; Sakai et al., 1996). I assume that carp RDH8L2 plays a similar role as mammalian RDH12 in the IS.

RDH13 localized in the IS, but accounted for a little of the RDH activity in the IS. Similarly as in the case of RDH8L2, the total expression level of RDH13 is several times higher in the CIS than in the RIS (Figure 14E), which would be because of a larger volume of the CIS. Therefore, the concentration of RDH13 could be similar between the RIS and

the CIS. The specific activity of RDH13 was much lower than that of RDH8 (Figure 15B). It has been reported that RDH13 is present in mitochondria in prostate cancer LNCaP cells (Belyaeva et al., 2008), but its function is not clear yet.

Cone-specific Retinal-Retinol Redox Coupling Reaction

11-*cis* retinal is directly supplied from the RPE to the OS of rods and cones. As discussed by Mata et al. (2002), this supply does not seem to fully support the amount of 11-*cis* retinal necessary to regenerate pigment in cones which function under bright light. The supply of 11-*cis* retinal from the RPE is estimated to be 28 pmols per minute per eye in chicken (Mata et al., 2002). From our determination, one carp retina contained 4.04 ± 1.84 nmols (n=7) of rod pigment and 0.04 nmols of cone pigment (cone cells contain 1/50 of rod cells in retinal homogenate). Assuming that a similar amount of 11-*cis* retinal is supplied from the RPE in carp as in chicken, its supply to each visual pigment in carp is calculated to be 1.1 x 10^{-4} 11-*cis* retinal/pigment-sec (28 pmols/4.08 nmols/60sec). Based on this calculation, the rate of supply of 11-*cis* retinal from the RPE to carp retina becomes insufficient when cones are exposed to light bleaching >0.01% of visual pigment bleached /sec, above which intensities cones operate normally (for example, see Burkhardt, 1994). This rate, however, could be overestimated in cones because the position of the COS is further away from the RPE than the ROS under light-adapted conditions.

Müller cells can produce 11-*cis* retinol, and cones can be regenerated by application of 11-*cis* retinol. Based on these facts, it has been proposed that 11-*cis* retinol supplied from Müller cells is converted to 11-*cis* retinal in cones and that this mechanism is a cone-specific additional visual cycle pathway to provide 11-*cis* retinal to cones effectively (Mata et al., 2002; Muniz et al., 2007). It has been postulated that 11-*cis* retinol dehydrogenase, which converts 11-*cis* retinol to its retinal in the presence of $NADP^+$, is responsible for this reaction.

In the present study, however, as I showed in Figure 7B, this activity was low in purified carp cones. The rate was 0.065 ± 0.020 amols 11-*cis* retinal/cone-sec. In the presence of NAD^+, instead of $NADP^+$, the conversion of 11-*cis* retinol to 11-*cis* retinal was 4 times less effective than in the presence of $NADP^+$. In contrast to this low activity, the higher

rate of the conversion of 11-*cis* retinol to 11-*cis* retinal was observed by the ALOL coupling in the absence of the cofactor, $NADP^+$: the rate was 3.5 ± 0.3 amols of 11-*cis* retinal (equal to all-*trans* retinol) formed/cone-sec (Figure 20) and it was 50 (3.5/0.065) times higher than the rate of production of 11-*cis* retinal attained by the postulated 11-*cis* retinol dehydrogenase activity. Therefore, the ALOL coupling is a very effective mechanism to produce 11-*cis* retinal from its retinol that is supplied from Müller cells.

If the activity of the ALOL coupling all resides in the COS, the maximal rate of coupling is equal to 0.027 ± 0.002 11-*cis* retinal formed/pigment-sec. At the maximal rate of production of 11-*cis* retinal by the coupling, the activity is >240 times ($0.027/(1.1 \times 10^{-4})$) higher than the supply of 11-*cis* retinal from the RPE. The rate of the supply of 11-*cis* retinal by the coupling suggests that the supply is sufficient up to the light intensity bleaching 2.7% of pigment/sec.

Although the ALOL coupling provides 11-*cis* retinal in cones very effectively, this mechanism probably functions only under bright light. As shown in Figure 20, the K_m of this reaction to all-*trans* retinal is rather high (33 μM). All-*trans* retinal released from opsin after bleach probably binds to the cone membranes, and therefore, the local concentration of all-*trans* retinal could be higher than that calculated simply from the intensity of bleaching light and the pigment concentration in cones. The fact that visual pigment was regenerated by using endogenously produced A2 all-*trans* retinal (Figure 19) suggests that it could be the case. However, even if it is the case, the concentration of all-*trans* retinal would be still lower than its K_m value when the light intensity is low. I speculate that under these conditions, the supply of 11-*cis* retinal from the RPE is the main pathway and that the ALOL coupling becomes a major reaction when the light intensity increased to produce a large amount of all-*trans* retinal. The ALOL coupling does not require $NADP^+$ for the oxidation of 11-*cis* retinol, which suggests that cone pigments can be regenerated even when this cofactor, which is produced in the OS in an energy-dependent way (Hsu and Molday, 1994), runs out in the COS.

On the other hand, 11-*cis* retinol is also necessary for the ALOL coupling. I roughly quantified the amount of 11-*cis* retinol in the purified cones and rods by retinoid analysis with HPLC. Assuming that the pigment concentration is 3mM (Harosi, 1975), 11-*cis* retinol

concentration is calculated to be tens of times higher in cones than in rods, 800 μM (n=1) in cones and 20 μM (n=2) in rods. This result suggested that 11-*cis* retinol is transported from the Müller cells much preferably to cones, and that the coupling reaction probably could function as a mechanism to supply 11-*cis* retinal to cone opsin.

I showed that the reduction of all-*trans* retinal and the oxidation of 11-*cis* retinol are coupled with 1:1 stoichiometry (Figure 18D and 18E). Because 11-*cis* retinal is necessary for visual pigment regeneration and all-*trans* retinal is toxic to cells, the coupling reaction would be very useful for photoreceptor cells to remove toxic aldehyde.

Figure 21 summarizes the visual cycle for rods and cones. The cycle for rods (left) is adopted from those suggested previously (McBee et al., 2001; Lamb and Pugh, 2004), and that for cones (right) was drawn based on the scheme similar to that for rods with addition of our present finding (red and blue arrows).

As I showed in the present study, the ALOL coupling is probably catalyzed by an enzyme, because the activity was lost by heat treatment (Figure 18H). This activity is present in the cone membranes. The entity of this enzyme has not been identified yet. Because the dissociation constants of 11-*cis* and all-*trans* retinoids are different (Figure 7B), this reaction is not due to $NADP^+$/NADPH-dependent RDHs. In fact, in the absence of $NADP^+$/NADPH, this coupling reaction was observed. Furthermore, our expressed RDH8, RDH8L2, RDH13, or RPE containing RDH5 abundantly did not show this activity (data not shown). It could be the case that the enzyme is the one that has not been known previously or that the known RDHs require a protein(s) that is expressed specifically in cones.

There are many other issues to be answered. For example, the transport mechanism of 11-*cis* retinol from Müller cells to cones, is not known. It is only assumed that Interphotoreceptor retinol binding protein (IRBP) has a role to transport 11-*cis* retinol. Because Müller cells are present in the proximal part of the outer limiting membrane, they are spatially not close to cone outer segment. On the other hand, the site where cone pigment is regenerated is the cone outer segment. It is not known yet to which part of cones 11-*cis* retinol is transported and in which part of cones the ALOL coupling takes place. Further studies are obviously required to clarify these issues.

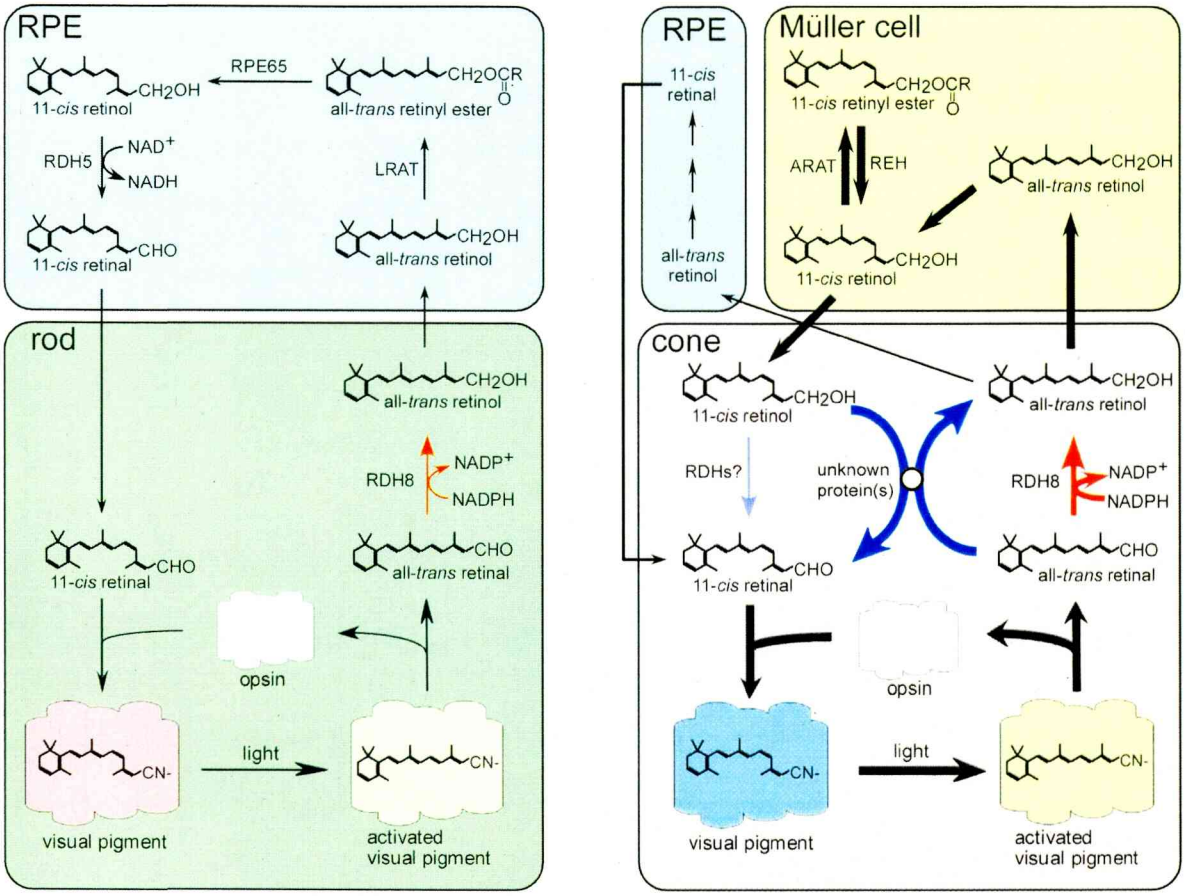

Figure 21. Proposed model of rod and cone visual cycle. The present study proposed the details of two steps of visual cycle. Firstly, all-*trans* retinal detached from opsin is reduced by RDH8 to all-*trans* retinol in rods and cones (red arrow). Secondly, 11-*cis* retinol supplied from Müller cells is converted to 11-*cis* retinal by the ALOL coupling reaction without a cofactor, $NADP^+$ (blue arrow). See text for details.

Experimental Procedures

Purification of Rod and Cone Photoreceptor Cells

Carp (*Cyprinus carpio*) rods and cones were isolated as described (Tachibanaki et al., 2005). The collected rods and cones were washed additionally with a K-gluconate (K-gluc) buffer (115 mM K-gluc, 2.5 mM KCl, 2 mM $MgCl_2$, 0.2 mM EGTA, 0.1mM $CaCl_2$, 1 mM DTT, 10mM Hepes, pH7.5) by centrifugation (600 x g for 12 sec, and then 3000 x g for 4 sec). In most of purified rods and cones (both >90%), the inner segment (IS) was attached to the outer segment (OS). The purified rods and cones lacked nucleus and terminal regions.

Preparation of Outer Segment-Rich and Inner Segment-Rich Rods and Cones

To prepare a rod outer segment (ROS)-rich and inner segment (RIS)-rich samples, purified rods were suspended in a Ringer's solution (119.9 mM NaCl, 2.6mM KCl, 0.5 mM $CaCl_2$, 0.5 mM $MgCl_2$, 0.5 mM $MgSO_4$, 1 mM $NaHCO_3$, 16 mM glucose, 0.5 mM NaH_2PO_4, 4 mM Hepes, pH 7.5) and passed through a 27-gauge needle several times with a 1-ml syringe to mechanically detach the OS from the IS. The suspension was layered on the top of a stepwise Percoll density gradient (30/45/60/90% (w/v)) and centrifuged at 10,000 x g for 20 min. At the interface between 30% and 45% Percoll, ROSs with or without RIS were found. This fraction was collected as the ROS-rich fraction. At the interface between 45% and 60% Percoll, RISs with or without ROS were found. This fraction was collected as the RIS-rich fraction. Each fraction was washed with the Ringer's solution and additionally with a K-gluconate (K-gluc) buffer, similar to purified rods and cones as described (Tachibanaki et al., 2005).

The purified cones were similarly passed through a 27-gauge needle. The suspension was centrifuged at 600 x g for 1 min. The cone outer segment (COS)-rich fraction was obtained as the supernatant, and the cone inner segment (CIS)-rich fraction was obtained as the precipitate. The COS-rich fraction was further centrifuged (124,000 x g for 20 min) to condense the fraction. The visual pigment content and the dehydrogenase activity were also measured.

The content of the IS in OS- and IS-rich preparations was estimated by comparing the

activity of mitochondrial succinate dehydrogenase (see below) as a marker of the IS and the amount of visual pigment as a marker of the OS. The ratio of IS/OS in the purified rod or cone preparation was taken to be 1, because most of purified rods and cones possessed both the OS and the IS (see above).

All of the preparations were frozen with liquid nitrogen and then stored in the dark at -80 °C until use.

Measurement of Succinate Dehydrogenase Activity in Rod and Cone Preparations

The measurement of succinate dehydrogenase (SDH) activity was carried out as described (Ackrell et al., 1978) with slight modifications. A rod or a cone preparation was suspended in 200 μl of Tris-HCl buffer (20 mM Tris, 0.1 mM EDTA, pH 7.5). The lysate contained 0.3-1 μM rod pigment or 0.003-0.04 μM cone pigment. SDH assay was initiated by adding 50 μl of 200 mM sodium succinate (pH 7.5) and 10 μl of 10 mM potassium ferricyanide, and the mixture was incubated at 25 °C. The absorbance decrease by reduction of ferricyanide by SDH was measured at 420 nm. The activity was determined at 200-500 seconds after the ferricyanide addition, and is expressed as the rate of reduction of ferricyanide in units of fmols of ferricyanide reduced per OS per second.

Preparation of Retinoids

All-*trans* retinal and all-*trans* retinol were purchased from Sigma. 11-*cis* retinal was prepared from all-*trans* retinal as described (Matsumoto et al., 2003) using 880 HPLC System (JASCO) equipped with a preparative Develosil column (Develosil 60-5, Nomura Chemical). 11-*cis* retinol was prepared by reduction of 11-*cis* retinal with $NaBH_4$ in ethanol, extracted in dichloromethane and *n*-hexane (Suzuki and Makino-Tasaka, 1983), and purified by HPLC with the method used for identification of retinal and retinol isomers (see below). All the retinoids were dissolved in ethanol and stored in the dark at -80 °C until use. Their purity was checked by examining an absorption spectrum (Garwin and Saari, 2000) prior to each experiment.

Measurements of Reduction or Oxidation of Retinoids

Purified rods or cones kept at -80 °C were lysed at room temperature and suspended in 100 μl of the K-gluc buffer. The lysate contained 0.25-0.5 μM rod pigment or 0.1-0.25 μM cone pigment. The measurements were carried out as described (Palczewski et al., 1994; Jang et al., 2000; Sun et al., 2007) with slight modifications. Reduction of all-*trans* retinal was initiated by adding 1 μl of NADPH (final concentration, 200 μM) and 1 μl of all-*trans* retinal dissolved in ethanol (final concentration, 100 μM) to 100 μl of the sample. The sample was incubated at room temperature for desired time, and the reaction was terminated by adding 150 μl of ice-chilled methanol. Reduction of 11-*cis* retinal was carried out similarly. Oxidation of retinols was initiated by addition of 1 μl of $NADP^+$ (final concentration, 200 μM) and 1 μl of all-*trans* or 11-*cis* retinol (final concentration, 100 μM). In the measurement of the retinal-retinol redox coupling reaction (ALOL coupling, see text), oxidation of 11-*cis* retinol was carried out in the absence of $NADP^+$, but in the presence of all-*trans* retinal under similar conditions used for the measurements in the presence of $NADP^+$.

Retinols were extracted directly and retinals were extracted as retinal-oximes after incubation with 50 mM NH_2OH on ice for 30 min with dichloromethane and *n*-hexane as described (Suzuki and Makino-Tasaka, 1983) with slight modifications. The extract was dissolved in a hexane solution containing 5% (v/v) *tert*-butylmethylether, 25% (v/v) benzene, 0.04% (v/v) ethanol. Each retinoid or retinal-oxime was separated by HPLC using a normal phase HPLC column (Cosmosil 5SL-II, Nacalai Tesque) at a flow rate of 0.5 ml/min of the above hexane solution as described (Irie and Seki, 2002) with a slight modification. The elution of a retinoid was monitored at 325 nm. The isomer type was identified by the retention time and the absorption spectrum. Retinols were directly quantified and retinals were quantified as retinal-oximes.

Cloning of RDH Genes

The partial coding region of each RDH was amplified from the carp retinal cDNA library (Shimauchi-Matsukawa et al., 2005) by PCR with a pair of primers. The sequences of the primers are shown in Table 1. The nucleotide sequences of the RDH cDNA clones were determined with an PRISM 3130 Genetic Analyzer (Applied Biosystems).

For determination of the full-length nucleotide sequences of RDH8, RDH8L2 and RDH13, DIG-labelled riboprobes were synthesized to screen the carp retinal cDNA library (GenBank accession numbers: RDH8, AB439579; RDH8L2, AB439580; RDH13, AB439581).

Table 1. Primers used for RDH cDNA cloning*

Gene name	Forward primer	Reverse primer
RDH5	ATHCARAARGCNATGGARTGG	ARNGCRTGYTCCATRCARTT
RDH8 RDH8L2 RDH8L3	GTNTAYGCNACNATGMG	CCYTCNACNGCRAAYTT
RDH12 RDH12L RDH12L2 RDH13 RDH14	GGNATHGGNAARGARAC	ACNCCNGCRTTRTTDAT
RDH13L	GGNATHGGNAARGARAC	WCRAAYTGCATYTCRAA
retSDR1 retSDR1L	GAATTCATGGATCTGAAGGCGC	CTCGAGTCATGTCCGCCCCTTG

*The partial coding region of each RDH was amplified from the carp retinal cDNA by PCR with a pair of primers shown.

Phylogenetic Analysis

Phylogenetic analysis was carried out as described (Shimauchi-Matsukawa et al., 2005). Amino acid sequences of the vertebrate RDHs were aligned with Clustal W. A total of 173 confidently aligned residues were used for estimating relationships among the proteins with the neighbor-joining method using the PHYLIP version 3.5c software package. For carp RDH8, RDH8L2 and RDH13, the entire nucleotide sequences were determined. However, there were genes that were only partially sequenced, and these genes did not contain the region used for the comparison. In this case, I used the amino acid sequence of the corresponding RDH gene of zebrafish for the analysis. The amino acid identity was determined by comparing the sequenced region of the carp gene and the corresponding region of the zebrafish gene. The vertebrate RDHs used are shown in Table 2.

Table 2. Vertebrate RDHs used for phylogenetic analysis

Species	Name in Figure 12A	Accession number	Definition in the DDBJ
carp	RDH8	AB439579	retinol dehydrogenase 8
	RDH8L2	AB439580	retinol dehydrogenase 8 like 2
	RDH13	AB439581	retinol dehydrogenase 13
zebrafish	RDH5	NP_001025272	retinol dehydrogenase 5
	RDH8	NP_957001	retinol dehydrogenase 8
	RDH8L	NP_957082	retinol dehydrogenase 8 like
	RDH8L2	XP_684476	PREDICTED: similar to MGC84258 protein
	RDH8L3	NP_001018379	hypothetical protein LOC553564
	RDH12	NP_001002325	retinol dehydrogenase 12 (all-trans and 9-cis)
	RDH12L	NP_001009912	retinol dehydrogenase 12, like
	RDH12L2	NP_001018519	hypothetical protein LOC553712
	RDH13	XP_691526	PREDICTED: hypothetical protein
	RDH13L	XP_698537	PREDICTED: similar to LOC407663 protein
	RDH14	NP_001040655	retinol dehydrogenase 14
	retSDR1	NP_001003477	dehydrogenase/reductase (SDR family) member 3
	retSDR1L	NP_001006070	hypothetical protein LOC450050
mouse	RDH5	NP_598767	retinol dehydrogenase 5
	RDH8	NP_001025461	retinol dehydrogenase 8
	RDH11	NP_067532	retinol dehydrogenase 11
	RDH12	NP_084293	retinol dehydrogenase 12
	RDH13	NP_780581	retinol dehydrogenase 13 (all-trans and 9-cis)
	RDH14	NP_076186	alcohol dehydrogenase PAN2 (RDH14)
	retSDR1	NP_035433	dehydrogenase/reductase (SDR family) member 3
human	RDH5	NP_002896	retinol dehydrogenase 5 (11-cis and 9-cis)
	RDH8	NP_056540	retinol dehydrogenase 8 (all-trans)
	RDH11	NP_057110	retinol dehydrogenase 11
	RDH12	NP_689656	retinol dehydrogenase 12 (all-trans and 9-cis)
	RDH13	NP_612421	retinol dehydrogenase 13
	RDH14	NP_065956	retinol dehydrogenase 14 (all-trans and 9-cis)
	retSDR1	NP_004744	dehydrogenase/reductase (SDR family) member 3

Measurement of the Expression Level of RDH mRNA with Real-time RT-PCR

Total RNA was extracted from the retina and the RPE of three individual carp, and cDNA was synthesized as described (Shimauchi-Matsukawa et al., 2005) with a slight modification. Briefly, after DNase I (Invitrogen) treatment, first-strand cDNA was synthesized with SuperScript III (Invitrogen) using 2.5 μM random hexamers. The primers were designed with Primer Express Software version 2.0 (Applied Biosystems). The primer sequences used are shown in Table 3.

Real-time RT-PCR was performed using an ABI PRISM 7300 (Applied Biosystems) according to the manufacturer's protocol. All PCR reactions were performed in duplicate using cDNA obtained from three animals. Control measurements were done in the absence of reverse transcriptase showed that the levels of genomic DNA contaminants and the formation of primer-dimers were negligible. Data were calibrated using a standard curve generated from known amounts of the corresponding DNA obtained by PCR amplification. In each determination, the ratio of the amount of mRNA of each RDH to that of an endogenous reference (18S ribosomal RNA) was determined in the retina and the RPE.

Table 3 Primers used for Real-time RT-PCR*

	Forward primer	Reverse primer
RDH5	GACGATGGACTTCTTGCCTCTT	GCAATATCCTCCGCCGTTAG
RDH8	CGAGCTGGCCACATAATCGT	AGAAGCCCTCTATGGCAAACTTAG
RDH8L2	AGGGCAACTACCCATAGATGCA	CATTCTCCTGTGAAATATGCGTAGA
RDH8L3	ATTGGCCCCATTGAGTGTCA	TATCAGGCAGAATCTCCTTCAAGAG
RDH12	CTTTGGATTTGGCCTTTCGA	CCACCTACTCGTGTACGGATCTC
RDH12L	AGCCATAAACCTGGCAAAGAGA	CTTTACTTCCTTCAGGGCTGCTT
RDH12L2	AGTCATCATGGCCTGTCGAGAT	ATCAAGTTTGTTCGCCACAATG
RDH13	CCACAGGAAATGGCAATGTAGTC	CCAGTCGTTCTTCTGTTGCTATGA
RDH13L	CTGGCCTCCTTGCAGTCTGT	GGCACATCATTATCCCAGCATT
RDH14	GGCGGCCCAGGACATC	GCAGAAGCTGCGCACAGA
retSDR1	TGCGCGTTGCTTTTTCCT	CCAGTGATGAGGACCACATCAG
retSDR1L	TACAAGCAAGCCAAGGTTGTCA	CATCACTGTCGAGCAAACTCTTTC
18S rRNA	TCATTCCGATAACGAACGAGACT	GTGGCTGAACGCCACTTGT

*Each sequence used for a semi-quantitative RT-PCR reaction was verified by BLAST search that the sequence is unique to the target RDH.

Preparation of Anti-RDH8, RDH8L2 and RDH13 Polyclonal Sera

Partial sequences of RDH8, RDH8L2 and RDH13 genes corresponding to 196-318, 192-310 and 282-329 aa residues (Figure 13A), respectively, were cloned into *Eco*RI-*Xho*I sites in pGEX-5X-1 vector (GE Healthcare). The recombinant plasmids coded the N-terminus GST-fused RDH peptides. They were introduced into *E. coli* (BL21DE3), and the recombinant partial peptides were expressed by induction with 1 mM isopropyl-1-thio-ß-galactopyranoside (IPTG) and purified with a glutathione resin column (GE Healthcare). Anti-RDH8, RDH8L2 and RDH13 antisera were raised against the each purified GST fused peptide in mice.

Quantification of RDH Proteins

Recombinant RDH8, RDH8L2 and RDH13 were used as standards to obtain a calibration curve in quantification of these RDHs (Figures 13 and 14). RDH8L2 and RDH13 were expressed in *E. coli*, but RDH8 was expressed in Sf9 cells for a reason shown below.

The coding region of RDH8L2 was cloned into *Nco*I-*Bam*HI sites in pQE70 vector (Qiagen). The recombinant plasmid coded the C terminus 6xHis-tag-fused RDH8L2. The 6xHis-tagged RDH8L2 was expressed in *E. coli* (BL21DE3), purified on a nickel-charged resin (Ni-NTA agarose, Qiagen), and used for quantification. The coding region of RDH13 was cloned into *Eco*RI-*Bam*HI sites in pMAL-c2X vector (New England Biolabs). The recombinant plasmid coded the N-terminus maltose binding protein (MBP)-fused RDH13. MBP-fused RDH13 was expressed in *E. coli* and purified on an amylose resin column (New England Biolabs). The MBP region was removed by Factor Xa (New England Biolabs).

On an SDS-PAGE, the protein band of endogenous RDH8 was close to that of rod pigment, and was masked with a very heavy band of this pigment. For this, I intended to obtain a calibration curve in the presence of rod pigment of similar amount present in the rod sample. At first RDH8 expressed in *E. coli* as a MBP-fusion protein was used. When MBP was removed, this *E. coli* recombinant showed a band at a higher molecular mass on an SDS-PAGE than that of the endogenous RDH8, and therefore, that of rod pigment. It was probably because the cleavage by Factor Xa was improperly made. Because of separation of the protein band of RDH8 expressed in *E. coli* and that of rod pigment, quantification of endogenous RDH8 was not possible.

Recombinant RDH8 was then expressed in Sf9 cells. This recombinant protein was similar to carp native RDH8 on an SDS-PAGE, and therefore, it could be used for quantification. The coding region of RDH8 was cloned into *Eco*RI-*Xho*I sites in pFastBac1 vector (Invitrogen). To produce baculoviruse, first the pFastBac1 vector was transformed into DH10Bac competent cells (Invitrogen). Positive clones were selected and the insert was checked by the PCR method. Sf9 cells (Invitrogen) were transfected with the purified Bacmid using Cellfectin Reagent (Invitrogen). After transfection, the supernatant was collected as a virus stock. Sf9 cells were cultured in Sf-900 II SFM (Intitrogen) at 27 °C. Cells were plated on

a culture dish of 10 cm diameter and infected with the recombinant baculovirus. Two days after infection, the cells were collected from one dish, washed with an ice-chilled phosphate-buffered saline (2 mM KH_2PO_4, 10 mM Na_2HPO_4, 137 mM NaCl, 2.7 mM KCl, pH 7.5; PBS) and homogenized in the K-gluc buffer on ice. Cell lysate was used for quantification of RDH8. RDH8L2 and RDH13 were similarly expressed in Sf9 cells by cloning into *Eco*RI-*Xho*I sites (RDH8L2) and *Bam*HI-*Hind*III sites (RDH13) in pFastBac1 vector.

For quantification of RDH8, RDHL2 and RDH13, I detected their immunoblot signals and compared them with calibration curves made with known amounts of Sf9 recombinant RDH8 and the *E. coli* recombinant RDH8L2 and RDH13. In the case of rods, rod pigment purified as reported previously (Okano et al., 1989) was added to RDH8 at the same amount that was present in the rod sample.

Measurement of specific activities of RDH8, RDH8L2 and RDH13

In previous studies, RDH activities in recombinant proteins were measured with proteins expressed in HEK293 cells (Jang et al., 2000; Sun et al., 2007). In our present study, I also used RDH8, RDH8L2 and RDH13 expressed in this culture cell line. The coding region of RDH8, RDH8L2 or RDH13 was cloned into *Eco*RI-*Xho*I, *Kpn*I-*Bam*HI or *Not*I-*Sal*I sites in a pEF-BOS-EX vector, respectively (Mizushima and Nagata, 1990). HEK293 cells were cultured in minimal essential medium containing 10% fetal bovine serum at 37 °C with 5% CO_2. Cells were plated on 35mm dishes and transiently transfected with expression constructs for RDH8, RDH8L2 or RDH13 in a pEF-BOS-EX vector using FuGENE HD transfection Reagent (Roche Diagnostics). Two days after transfection, the cells were collected from one dish, washed with ice-chilled PBS. The cells were suspended with 300 μl of the K-gluc buffer and stored at -80 °C until use. Cell lysate was centrifuged at 20,000 x g for 15 min at 4 °C, and the precipitate was used for the measurement of RDH activities. The amount of the expressed protein was calibrated by immunoblots.

Measurement of Visual Pigment Regeneration by 11-*cis* Retinal Formed from 11-*cis* Retinol in Cones

The lysate of purified cones containing 1.7 μM cone visual pigment (final concentration)

was suspended in 500 μl of the K-gluc buffer. The sample was divided into five portions, 100 μl each. The endogenous 11-*cis* retinal in carp is a derivative of vitamin A2 (A2 11-*cis* retinal). A2 11-*cis* retinal was converted to A2 all-*trans* retinal by bleaching the red pigment (λ_{max} = ~620 nm) completely with a 100 W projector lamp with a cut-off filter passing light longer than 680nm at room temperature for 5 min. To each portion, various manipulations were made depending on the purpose of the study (see text). Each portion was sedimented by centrifugation (124,000 x g for 20 min), and the precipitate containing cone membranes was incubated at room temperature for 10 min in the dark to allow regeneration of cone pigments. When necessary, 1 μ l of 11-*cis* retinal solution in ethanol (final concentration: 10 μM), 11-*cis* retinol solution in ethanol (final concentration: 2 μM), NH_2OH solution (final concentration: 20 mM) or NADPH solution (final concentration: 200 μM) was added to the sample.

After incubation, all samples were suspended in an extraction buffer containing 0.75% (w/v) 3-[(3-cholamidopropyl) dimethylammonio]-1-propanesulfonate, 1 mg/ml phosphatidylcholine, 50 mM Hepes, 140 mM NaCl, 2 mM $MgCl_2$, 20% (w/v) glycerol, and 1 mM dithiothreitol ; pH 7.5). After extraction, the absorption spectrum of each portion was measured in the dark. To quantify the amount of red pigment regenerated (λ_{max} = ~570 nm), I illuminated the sample with >680nm light for 2-3 hours to fully bleach the red pigment, and then the absorption spectrum was measured again. The spectrum measured after the bleach was subtracted from that measured in the dark (difference spectrum) to quantify the amount of red pigment regenerated.

References

Ackrell, B.A., Kearney, E.B., and Singer, T.P. (1978). Mammalian succinate dehydrogenase. Methods. Enzymol. *53*, 466-483.

Ala-Laurila, P., Kolesnikov, A.V., Crouch, R.K., Tsina, E., Shukolyukov, S.A., Govardovskii, V.I., Koutalos, Y., Wiggert, B., Estevez, M.E., and Cornwall, M.C. (2006). Visual cycle: Dependence of retinol production and removal on photoproduct decay and cell morphology. J. Gen. Physiol. *128*, 153-169.

Baylor, D.A., Nunn, B.J., and Schnapf, J.L. (1984). The photocurrent, noise and spectral sensitivity of rods of the monkey Macaca fascicularis. J. Physiol. *357*, 575-607.

Belyaeva, O.V., Korkina, O.V., Stetsenko, A.V., Kim, T., Nelson, P.S., and Kedishvili, N.Y. (2005). Biochemical properties of purified human retinol dehydrogenase 12 (RDH12): catalytic efficiency toward retinoids and C9 aldehydes and effects of cellular retinol-binding protein type I (CRBPI) and cellular retinaldehyde-binding protein (CRALBP) on the oxidation and reduction of retinoids. Biochemistry *44*, 7035-7047.

Belyaeva, O.V., Korkina, O.V., Stetsenko, A.V., and Kedishvili, N.Y. (2008). Human retinol dehydrogenase 13 (RDH13) is a mitochondrial short-chain dehydrogenase/reductase with a retinaldehyde reductase activity. FEBS J. *275*, 138-147.

Burkhardt, D. A. (1994). Light adaptation and photopigment bleaching in cone photoreceptors in situ in the retina of the turtle. J. Neurosci. *14*, 1091-1105.

Burns, M.E., and Arshavsky, V.Y. (2005). Beyond counting photons: Trial and trends in vertebrate visual transduction. Neuron *48*, 387-401.

Calvert, P.D., Govardovskii, V.I., Arshavsky, V.Y., and Makino, C.L. (2002). Two temporal phases of light adaptation in retinal rods. J. Gen. Physiol. *119*, 129-145.

Chang, H., and Gilbert, W. (1997). A novel zebrafish gene expressed specifically in the photoreceptor cells of the retina. Biochem. Biophys. Res. Commun. *237*, 84-89.

Das, S.R., Bhardwaj, N., Kjeldbye, H., and Gouras, P. (1992). Müller cells of chicken retina synthesize 11-*cis* retinol. Biochem. J. *285*, 907-913.

Dowling, J.E., and Boycott, B.B. (1966). Organization of the primate retina: electron microscopy. Proc. R. Soc. Lond. B. Biol. Sci.. *166*, 80-111.

Eldred, G.E., and Lasky, M.R. (1993). Retinal age pigments generated by self-assembling lysosomotropic detergents. Nature *361*, 724-726.

Fu, Y., and Yau, K.W. (2007). Phototransduction in mouse rods and cones. Pflugers Arch. *454*, 805-819.

Futterman, S. (1963). Metabolism of the retina. III. The role of reduced triphoshopyridine nucleotide in the visual cycle. J. Biol. Chem. *238*, 1145-1150.

Garwin, G.G., and Saari, J.C. (2000). High-performance liquid chromatography analysis of visual cycle retinoids. Methods. Enzymol. *316*, 313-324.

Gether, U. (2000). Uncovering molecular mechanisms involved in activation of G protein-coupled receptors. Endocr. Rev. *21*, 90-113.

Goldstein, E.B., and Wolf, B.M. (1973). Regeneration of the green-rod pigment in the isolated frog retina. Vision Res. *13*, 527-534.

Groenendijk, G.W., Jacobs, C.W., Bonting, S.L., and Daemen, F.J. (1980). Dark isomerization of retinals in the presence of phosphatidylethanolamine. Eur. J. Biochem. *106*, 119-128.

Haeseleer, F., Huang, J., Lebioda, L., Saari, J.C., and Palczewski, K. (1998). Molecular characterization of a novel short-chain dehydrogenase/reductase that reduces all-*trans*-retinal. J. Biol. Chem. *273*, 21790-21799.

Haeseleer, F., Jang, G.F., Imanishi, Y., Driessen, C.A., Matsumura, M., Nelson, P.S., and Palczewski, K. (2002). Dual-substrate specificity short chain retinol dehydrogenases from the vertebrate retina. J. Biol. Chem. *277*, 45537-45546.

Harosi, F.I. (1975). Absorption spectra and linear dichroism of some amphibian photoreceptors. J. Gen. Physiol. *66*, 357-382.

Hsu, S.C., and Molday, R.S. (1994). Glucose metabolism in photoreceptor outer segments. Its role in photo*trans*duction and in NADPH-requiring reactions. J. Biol. Chem. *269*, 17954-17959.

Irie, T., and Seki, T. (2002). Retinoid composition and retinal localization in the eggs of teleost fishes. Comp. Biochem. Physiol. B Biochem. Mol. Biol. *131*, 209-219.

Jang, G.F., McBee, J.K., Alekseev, A.M., Haeseleer, F., and Palczewski, K. (2000). Stereoisomeric specificity of the retinoid cycle in the vertebrate retina. J. Biol. Chem. *275*, 28128-28138.

Jones, G.J., Crouch, R.K., Wiggert, B., Cornwall, M.C., and Chader, G.J. (1989). Retinoid requirements for recovery of sensitivity after visual-pigment bleaching in isolated

photoreceptors. Proc. Natl. Acad. Sci. USA *86*, 9606-9610.

Kawamura, S., and Tachibanaki, S. (2008). Rod and cone photoreceptors: Molecular basis of the difference in their physiology. Comp. Biochem. Physiol. A Mol. Integr. Physiol. *150*, 369-377.

Lamb, T.D., and Pugh, E.N. Jr. (2004). Dark adaptation and the retinoid cycle of vision. Prog. Retin. Eye Res. *23*, 307-380.

Lamb, T.D., and Pugh, E.N. Jr. (2006). Phototransduction, dark adaptation, and rhodopsin regeneration. The proctor lecture. Invest. Ophthalmol. Vis. Sci. *47*, 5137-5152.

Lee, S.A., Belyaeva, O.V., and Kedishvili, N.Y. (2008). Effect of lipid peroxidation products on the activity of human retinol dehydrogenase 12 (RDH12) and retinoid metabolism. Biochim. Biophys. Acta. *1782*, 421-425.

Maeda, A., Maeda, T., Imanishi, Y., Kuksa, V., Alekseev, A., Bronson, J.D., Zhang, H., Zhu, L., Sun, W., Saperstein, D.A., Rieke, F., Baehr, W., and Palczewski, K. (2005). Role of photoreceptor-specific retinol dehydrogenase in the retinoid cycle in vivo. J. Biol. Chem. *280*, 18822-18832.

Maeda, A., Maeda, T., Sun, W., Zhang, H., Baehr, W., and Palczewski, K. (2007). Redundant and unique roles of retinol dehydrogenases in the mouse retina. Proc. Natl. Acad. Sci. USA *104*, 19565-19570.

Mata, N.L., Radu, R.A., Clemmons, R.C., and Travis, G.H. (2002). Isomerization and oxidation of vitamin a in cone-dominant retinas: a novel pathway for visual-pigment regeneration in daylight. Neuron *36*, 69-80.

Matschinsky, F.M. (1968). Quantitative histochemistry of nicotinamide adenine nucleotides in retina of monkey and rabbit. J. Neurochem. *15*, 643-657.

Matsumoto, H., Nakamura, Y., Tachibanaki, S., Kawamura, S., and Hirayama, M. (2003). Stimulatory effect of cyanidin 3-glycosides on regeneration of rhodopsin. J. Agric. Food Chem. *51*, 3560-3563.

McBee, J.K., Palczewski, K., Baehr, W., and Pepperberg, D.R. (2001). Confronting complexity: the interlink of photo*trans*duction and retinoid metabolism in the vertebrate retina. Prog. Retin. Eye Res. *20*, 469-529.

Mendez, A., Burns, M.E., Sokal, I., Dizhoor, A.M., Baehr, W., Palczewski, K., Baylor, D.A., and Chen, J. (2001). Role of guanylate cyclase-activating proteins (GCAPs) in setting the flash

sensitivity of rod photoreceptors. Proc. Natl. Acad. Sci. USA *98*, 9948-9953.

Mizushima, S., and Nagata, S. (1990) pEF-BOS, a powerful mammalian expression vector. Nucleic Acids Res. *18*, 5322.

Muniz, A., Villazana-Espinoza, E.T., Hatch, A.L., Trevino, S.G., Allen, D.M., and Tsin, A.T. (2007). A novel cone visual cycle in the cone-dominated retina. Exp. Eye Res. *85*, 175-184.

Nicotra, C., and Livrea, M.A. (1982). Retinol dehydrogenase from bovine retinal rod outer segments. Kinetic mechanisms of solubilized enzyme. J. Biol. Chem. *257*, 11836-11841.

Okano, T., Fukada, Y., Artamonov, I.D., and Yoshizawa, T. (1989). Purification of cone visual pigments from chicken retina. Biochemistry *28*, 8848-8856.

Palczewski, K., Jäger, S., Buczylko, J., Crouch, R.K., Bredberg, D.L., Hofmann, K.P., Asson-Batres, M.A., and Saari, J.C. (1994). Rod outer segment retinol dehydrogenase: substrate specificity and role in phototransduction. Biochemistry *33*, 13741-13750

Rattner, A., Smallwood, P.M., and Nathans, J. (2000). Identification and characterization of all-*trans*-retinol dehydrogenase from photoreceptor outer segments, the visual cycle enzyme that reduces all-*trans*-retinal to all-*trans*-retinol. J. Biol. Chem. *275*, 11034-11043.

Saari, J.C., Garwin, G.G., Van Hooser, J.P., and Palczewski, K. (1998). Reduction of all-*trans*-retinal limits regeneration of visual pigment in mice. Vision Res. *38*, 1325-1333.

Sakai, N., Decatur, J., Nakanishi, K., and Eldred, G. (1996). Ocular age of pigment "A2-E": an unprecedented pyridinium bisretinoid. J. Am. Chem. Soc. *118*, 1559-1560.

Schnapf, J.L., Nunn, B.J., Meister, M., and Baylor, D.A. (1990). Visual transduction in cones of the monkey Macaca fascicularis. J. Physiol. *427*, 681-713.

Shimauchi-Matsukawa, Y., Aman, Y., Tachibanaki, S., and Kawamura, S. (2005). Isolation and characterization of visual pigment kinase-related genes in carp retina: polyphyly in GRK1 subtypes, GRK1A and 1B. Mol. Vis. *11*, 1220-1228.

Shimizu, T., Ishiguro, S., and Tamai, M. (1998). Isomerization of 11-*cis*-retinol to all-*trans*-retinol in bovine rod outer segments. J. Biochem. *123*, 953-958.

Stenkamp, R.E., Teller, D.C., and Palczewski, K. (2005). Rhodopsin: a structural primer for G-protein coupled receptors. Arch. Pharm. (Weinheim) *338*, 209-216.

Sun, W., Gerth, C., Maeda, A., Lodowski, D.T., Van Der Kraak, L., Saperstein, D.A., Héon, E., and Palczewski, K. (2007). Novel RDH12 mutations associated with Leber congenital amaurosis

and cone-rod dystrophy: biochemical and clinical evaluations. Vision Res. *47*, 2055-2066.

Suzuki, T., and Makino-Tasaka, M. (1983). Analysis of retinal and 3-dehydroretinal in the retina by high-pressure liquid chromatography. Anal. Biochem. *129*, 111-119.

Tachibanaki, S., Tsushima, S., and Kawamura, S. (2001). Low amplification and fast visual pigment phosphorylation as mechanisms characterizing cone photoresponses. Proc. Natl. Acad. Sci. USA *98*, 14044-14049.

Tachibanaki, S., Arinobu, D., Shimauchi-Matsukawa, Y., Tsushima, S., and Kawamura, S. (2005). Highly effective phosphorylation by G protein-coupled receptor kinase 7 of light-activated visual pigment in cones. Proc. Natl. Acad. Sci. USA *102*, 9329-9334.

Tachibanaki, S., Shimauchi-Matsukawa, Y., Arinobu, D., and Kawamura, S. (2007). Molecular mechanisms characterizing cone photoresponses. Photochem. Photobiol. *83*, 19-26.

Tsina, E., Chen, C., Koutalos, Y., Ala-Laurila, P., Tsacopoulos, M., Wiggert, B., Crouch, R.K., and Cornwall, M.C. (2004). Physiological and microfluorometric studies of reduction and clearance of retinal in bleached rod photoreceptors. J. Gen. Physiol. *124*, 429-443.

Wald, G., and Brown, P.K. (1953). The molar extinction of rhodopsin. J. Gen. Physiol. *37*, 189-200.

Weng, J., Mata, N.L., Azarian, S.M., Tzekov, R.T., Birch, D.G., and Travis, G.H. (1999). Insights into the function of Rim protein in photoreceptors and etiology of Stargardt's disease from the phenotype in abcr knockout mice. Cell *98*, 13-23.

A list of achievements

＜投稿論文＞

・"Highly efficient retinal metabolism in cones."
Sadaharu Miyazono, Yoshie Shimauchi-Matsukawa, Shuji Tachibanaki, and Satoru Kawamura
Proceedings of the National Academy of Sciences, in press.

＜学会発表＞

・「色素顆粒形成・分解の小胞輸送機構」
宮園貞治、河村悟、尾崎浩一
第５回光生物シンポジウム（島根）、2002.6.7.

・「色素顆粒形成・分解の小胞輸送機構の解明」
宮園貞治、河村悟、尾崎浩一
２００３年度日本動物学会近畿支部研究発表会（大阪）、2003.5.31.

・「ショウジョウバエ網膜の色素顆粒形成過程」
宮園貞治、河村悟、尾崎浩一
第６回光生物シンポジウム（北海道）、2003.9.16.

・「ショウジョウバエ網膜に存在する色素顆粒の精製と局在蛋白質の同定」
宮園貞治、河村悟、尾崎浩一
日本動物学会第７４回大会（北海道）、2003.9.18.

・「ショウジョウバエ網膜色素顆粒に存在する蛋白質の同定とその特性」
宮園貞治、河村悟、尾崎浩一
日本比較生理生化学会第２７回大会（東京）、2005.8.4-6.

・「ショウジョウバエ網膜色素顆粒に局在する蛋白質の機能」
宮園貞治、河村悟、尾崎浩一
日本動物学会第７６回大会（茨城）、2005.10.6.

・「ショウジョウバエ網膜色素細胞におけるレチノイド代謝経路」
尾崎浩一、宮園貞治、菅美昇、大野大地
日本比較生理生化学会第２８回大会（静岡）、2006.7.27-29.

・「ショウジョウバエ網膜における脂肪酸結合蛋白質（FBP）の機能」
尾崎浩一、宮園貞治、菅美昇、大野大地
日本動物学会第７７回大会（島根）、2006.9.22.

・「桿体と錐体とでのレチナールからレチノールへの還元反応の違い」
宮園貞治、松川淑恵、橘木修志、河村悟
日本動物学会第７７回大会（島根）、2006.9.22.

・"Phototransduction in carp cones : activation and recovery"
Satoru Kawamura, Shuji Tachibanaki, Daisuke Arinobu, NorihikoTakemoto, Sadaharu Miyazono
FASEB Summer Research Conference. The Biology and Chemistry of Vision (Colorado, USA), 2007.6.20.

・「桿体と錐体とでのレチナールからレチノールへの還元反応の違い」
宮園貞治、松川淑恵、橘木修志、河村悟
第１４回日本光生物学協会年会（奈良）、2007.7.31.

・「桿体と錐体とでのレチナールからレチノールへの還元反応の違い」
宮園貞治、松川淑恵、橘木修志、河村悟
日本動物学会第７８回大会（青森）、2007.9.20.

・「桿体・錐体視細胞の応答の違いを生み出す分子機構」
橘木修志、松川淑恵、有信大輔、宮園貞治、竹本訓彦、富塚順子、越谷祐貴、瀬野亜希、河村悟
視覚科学フォーラム第１２回研究会（大阪）、2008.8.28.

・「コイ錐体視細胞における高いレチノイド代謝活性」
宮園貞治、松川淑恵、橘木修志、河村悟
日本動物学会第７９回大会（福岡）、2008.9.6.

Acknowledgements

I am grateful to Prof. Satoru Kawamura for invaluable discussions and suggestions throughout this study. I am indebted to Dr. Shuji Tachibanaki and Dr. Yoshie Shimauchi-Matsukawa for helpful discussions and advices. I am grateful to Dr. Takaharu Seki (Osaka Kyoiku University) for providing retinoids, helpful discussion and excellent technical advice about HPLC. I am grateful to Prof. Koichi Ozaki (Shimane University) for helpful discussion and advice. I thank Prof. Shigekazu Nagata (Kyoto University) for kindly allowing us to use an expression vector for HEK293 cells, and Prof. Hiroshi Kanazawa (Osaka University) for his help in establishing the RDH expression system. I thank Prof. Akihiko Ogura, Prof. Hisato Kondoh and Prof. Nobuhiko Yamamoto for helpful discussion and critical reading of this thesis. Finally, I am indebted to all members of Kawamura laboratory for their useful discussions and supports.